SLOW WAVE STRUCTURES FOR TRAVELLING WAVE MASERS

by

Rajni Kant Desai

A thesis submitted to the Faculty of Graduate Studies and Research in partial fulfilment of the requirements for the degree of Master of Science (Electrical Communications).

Eaton Electronics Research Laboratory
McGill University
April 1961

TABLE OF CONTENTS

ABSTRACT

Comb and meander line structures, which have been used in travelling wave masers, have been modified for use with solenoids. A theory for the determination of the dispersion characteristics of these structures has been outlined. Various methods for modifying the characteristics of a slow wave structure to suit travelling wave maser applications are also discussed.

Propagation along open comb and meander line structures was studied in the L band. A method was developed for the direct measurement of group velocity. Experimental results indicated that both the modified comb and meander line structures could be used in travelling wave maser circuits in conjunction with solenoids.

ACKNOWLEDGEMENTS

The author wishes to thank Professor G.A. Woonton, Director of the Eaton Electronics Laboratory, for making the facilities of the Laboratory available to him, and for financial assistance during the research programme. Professor Woonton is to be thanked for suggestions and discussions and Professor G.W. Farnell for his guidance during initial parts of this work. Thanks are also due to Mr. V. Avarlaid and his staff, who helped in the fabrication of the slow wave structures.

The author is indebted to the World University Service of Canada for an initial scholarship which made this work possible. He also gratefully acknowledges the personal financial assistance from the Defence Research Board, during the last two years, under a Research Assistant appointment.

INTRODUCTION

During the past decade a number of microwave devices have been invented that have grown largely out of fundamental research in the field of radio and microwave spectroscopy. One such device is the Maser (microwave amplification by stimulated emission of radiation). Before the invention of the Maser, the Travelling Wave Tube with a noise temperature (see Appendix II) of approximately 1000°K was used for microwave communication. The parametric amplifier increased the sensitivity by a factor of ten, but it was left to the Maser to produce a noise temperature of the order of 10°K. Because of its inherent low noise, the Maser has stimulated new interest in the field of space communication and radio astronomy.

The Maser brought new complexity to the field of microwave engineering. Previous microwave devices such as magnetrons and klystrons were adequately explained by classical theory. The Maser, however, is essentially a quantum mechanical device and classical theory is incapable of providing a complete discussion and understanding.

An extensive literature on Masers is available[1]. Current interest lies in the three level solid state maser utilising a paramagnetic crystal. The source of energy, the pump frequency, is a microwave signal which disturbs the equilibrium of the magnetic system to obtain an emissive condition. When stimulated by the signal requiring amplification, the energy stored is emitted coherently. As far as the circuit for the signal frequency is concerned there are two types of masers. For a given volume of crystal the interaction with the magnetic field may be intensified by placing it in a resonant cavity. The first solid state masers developed were of the cavity type. The gain can also be increased by placing the crystal along a slow-wave structure, i.e. a structure propagating an electro-magnetic wave with

a group velocity much less than the speed of light. This increases the time for which the field can interact with the crystal. Such travelling wave masers have been designed more recently.

Travelling wave masers have certain distinct advantages over cavity masers. Greater gain and appreciably more bandwidth can be obtained from a travelling wave maser. The gain is inherently more stable as small fluctuations of material properties and magnetic field cause smaller fluctuations in gain. The amplified frequency band can be electronically tuned over a wide range, depending on the bandwidth of the slow-wave structure, by varying the magnetic field and the pump frequency. An important feature of the travelling wave maser is that it can be designed to provide non-reciprocal amplification and attenuation. The isolators and circulators used in cavity systems may then be eliminated, thus decreasing the overall noise of the maser. Development work and research these days is mostly concentrated on travelling wave masers.

At present only five known crystals are available for maser applications. Of these synthetic ruby (Cr in Al_2O_3) is best suited for travelling wave masers. It has a high chemical stability, a good thermal conductivity, low dielectric losses, a high dielectric constant (approximately ten) and can be grown as a large single crystal in any given orientation. In travelling wave masers it is necessary to fabricate the active material in long sections to close tolerances. This requires a hard and strong material for machining, another condition satisfied by ruby. Other possible materials are gadolinium ethyl sulphate, emerald (Cr doped beryl), potassium chromicyanide and titanium dioxide (rutile).

The chief merit of the three level solid state maser is its capability of very low noise amplification. The low noise is mainly due to its operation at liquid helium temperature so that thermal noise is at a minimum. Thus in a well designed maser most of the noise is due to random spontaneous

emission. Low bath temperatures are, however, also necessary to obtain long relaxation times and a large population difference between levels of the signal transition. Although some amplification at liquid air temperatures has been obtained it is not yet feasible to operate masers at these temperatures. Operation at liquid helium temperatures also reduces ohmic losses in the slow-wave structure.

The most important component of a travelling wave maser is the slow-wave structure. Due to the extensive research carried out on travelling wave tubes, a large number of structures have been investigated. The characteristics of a structure required for the two types of amplifiers is, however, quite different. Whereas a travelling wave amplifier requires a constant phase velocity, a travelling wave maser needs a constant group velocity in the operation band. The gain of a travelling wave maser is inversely proportional to the group velocity, so that a minimum slowing of the wave is necessary to provide sufficient gain. The design of a structure for travelling wave masers must be compatible with the requirement that the applied magnetic field must have specific orientations with respect to the signal and pumping, high frequency fields. A further restriction is that it must exhibit non-reciprocal properties to prevent regeneration in the maser.

Slow wave structures can also be used with advantage in resonance studies due to the wide frequency range possible in a single apparatus without adjustment. Narrow band sensitive circuits can be used for such purposes as line-shape studies, studies of spin diffusion and cross-relaxation where two or more signals at different frequencies are applied to the system and then separated. Measurement procedures are also simpler in a travelling wave spectrometer as compared to a cavity spectrometer. The signal need not be stabilised or locked to the cavity resonance and f.m. noise on the signal

source does not introduce noise in detector. However, absolute measurements are possible in cavities where the field configurations are simpler and well known.

SECTION I

THEORY OF THE TRAVELLING WAVE MASER

Part I - Historical Introduction

The development of the travelling wave maser closely parallels that of the travelling wave tube. When the cavity maser showed a limitation in bandwidth, the use of a slow-wave structure was natural. The first travelling-wave maser was developed by DeGrasse, Schulz Du-Bois and Scovil[2] at the Bell Telephone Laboratories in 1958, using a ruby loaded comb structure. A net gain of 23 db with a bandwidth of 25 Megacycles (Mc) centred at 6 kilo-megacycles was obtained. This is in comparison to the 2 Mc bandwidth obtained for cavity masers for the same gain. Following on these lines Chang, Cromack and Siegman[3] at Stanford designed a travelling wave maser using a ruby loaded meander line. A larger bandwidth was obtained at the expense of gain. Recently Okwit, Arams and Smith[6] have operated a tunable travelling wave maser in the L and S bands by dielectrically loading the comb structure. Emphasis was laid on the tuning range, i.e. the range over which the slow-wave structure is capable of producing gain. For a 15% tuning range a gain of less than 10 db was obtained. It was estimated that a structure at least 6 inches long would be required to provide a gain of 30 db. This length is much too large for a practical amplifier.

Part II - Gain and Bandwidth of a travelling wave maser

The amplification in a travelling wave maser is obtained from power transferred to the microwave circuit by coherent excitation of the paramagnetic spins due to the magnetic fields of the circuit. High gain can be achieved by increasing the length of interaction or by decreasing the velocity at which energy propagates through the crystal. There being a practical limit to the former, reasonable amplification is obtained by 'slowing' the electro-magnetic wave.

An electro-magnetic wave can be described by electric and magnetic field components of the type

$$H_y = H_{yo} \exp j(wt-kz) \qquad (1)$$

z denotes the space co-ordinate in the direction of propagation, $w/2\pi$ is the frequency, t the time and k the propagation constant defined in MKS units as

$$k^2 = w^2 \epsilon_o \mu_o \epsilon \mu_r \qquad (2)$$

For a medium with no dielectric interaction and small magnetic loss (see Appendix I)

$$\epsilon = 1 \qquad \text{and} \qquad \mu_r = 1-j\chi'' \qquad (3)$$

In most cases, the magnetic permeability μ_r depends upon the orientation of the magnetic field H; thus μ_r and χ'' are tensor quantities.

Then $$k = \frac{w}{c}\left(1-j\frac{\chi''}{2}\right)$$

The imaginary component of k in the above equation shows that the amplitude of the wave decreases exponentially. The power transmitted by the wave is proportional to the square of the field amplitudes and thus decreases according to

$$P(z) = P(0) \exp\left(-\frac{w\chi'' z}{c}\right) \tag{4}$$

This formula applies also to an inverted maser material in which χ'' takes on negative values and indicates an exponential increase in power as the signal traverses the crystal.

For maser materials $\chi'' \simeq -10^{-2}$, so that equation (4) suggests the signal should travel for a length of the order of 100 wavelengths in the maser material to have an appreciable gain. Since maser structural lengths of this order are quite impractical, it is necessary to enhance the interaction between the material and wave. This can be accomplished by slowing the propagation of the wave, with a suitable periodic guiding structure.

Consider a structure periodic in the z-direction and of cross-section A_s. For a length dz the energy content, in terms of the magnetic field, is (see Appendix I)

$$dE = \frac{1}{2} \mu_o dz \int_{A_s} H.H^* dA \tag{5}$$

where H^* denotes the complex conjugate of H. If absorption is low, the energy travels with group velocity v_g in the z-direction. The power crossing some fixed cross-section is therefore

$$P = \frac{dE}{dz} v_g \tag{6}$$

The above relation is derived for the case in which energy remains constant in the process of propagation. It is still correct, however, for the case in which energy changes slowly with distance. Power absorbed by the maser material is given by (see Appendix I)

$$dP = -\frac{1}{2} w_o \mu_o dz \int_{A_m} H.\chi''.H^* \, dA \tag{7}$$

where the integration is performed over the cross-section of the maser material A_m.

$$\text{Thus} \qquad \frac{dP}{P} = -\frac{w}{v_g} \frac{\int_{A_m} H.\chi''.H^* dA}{\int_{A_s} H.H^* dA} dz \tag{8}$$

If the maser material does not fill the whole cross section of the slow-wave circuit, χ'' must simply be replaced by a fraction $F\chi''$ ($F < 1$). The "filling factor" F indicates to what extent the interaction of the wave and material is reduced. The value of F may be smaller than unity for two reasons. First, the maser material does not fill the entire cross-section of the structure and second, the polarization of H is not such as to yield the strongest interaction with the χ'' tensor. More rigorously, F is defined as

$$F = \frac{\int_{A_m} H.\chi''.H^* dA}{\chi''_m \int_{A_s} H.H^* dA} \tag{9}$$

where χ''_m is the diagonalized χ'' tensor. Thus

$$\frac{dP}{P} = -\frac{w}{v_g} F \chi''_m \, dz \tag{10}$$

Integrating the above equation gives the gain G for a structure of length $z = \ell$ as

$$G = \frac{P(\ell)}{P(0)} = \exp\left[-\frac{w\ell}{v_g} F \chi''_m \right] \tag{11}$$

The gain in decibels is

$$G_{db} = 10 \log_{10} G = 27.3(-\chi''_m) F \frac{f\ell}{v_g} \tag{12}$$

where f is the signal frequency. The frequency variation of the gain is given by the frequency dependence of χ''. For maser materials, where the concentration of the paramagnetic ions is small, the line shape is Lorentzian.

For a Lorentzian line

$$\chi''(f) = \chi''(f_o) \left[1 + \left(\frac{2(f-f_o)}{\Delta f}\right)^2 \right]^{-1} \qquad (13)$$

assuming saturation is negligible and where f_o is the centre frequency of the line and Δf is the half power bandwidth. The bandwidth B of the travelling wave maser is defined as the frequency range over which the gain is greater than half its peak value. From equation (11) if G_m represents the peak gain,

$$B = \Delta f \sqrt{\frac{n\,2}{\ln G_m - \ln 2}}$$

$$B = \Delta f \sqrt{\frac{3}{G_{dbm} - 3}} \qquad (14)$$

For a gain $G = 10^2$, 10^3, 10^4 this formula indicates that the maser bandwidth B is the material bandwidth Δf reduced by a factor 2.4, 3.0, 4.5 respectively. The bandwidth may be increased beyond the limit (14) by exposing the maser crystal to a slightly non-uniform dc magnetic field. This added bandwidth is bought at the expense of either total gain or increased length of the structure.

Of great practical importance is the problem of gain fluctuations, because in many applications gain variations would deteriorate a system performance in the same way as noise. Most likely in practice, gain fluctuations are caused by fluctuations of χ'', the complex susceptibility exhibited by the material. χ'' may change due to changes in frequency and power of the saturating pump signal. The gain sensitivity, S_G, may be defined as the ratio of relative change in G to relative change in χ''. Thus from (11)

$$S_G = \frac{dG/G}{d\chi''/\chi''} = \ln G = 0.230G \qquad (15)$$

where $\ln$ is the natural logarithm.

For a gain $G = 10^2$, 10^3, 10^4, and a change of χ'' by one percent, the

gain changes by 4.6, 6.9, 9.2 percent, respectively. By comparison, in a cavity maser the product $B(G)^{\frac{1}{2}}$ is a constant, at least for high gain, and $S_G = (G)^{\frac{1}{2}}$, so that for the above example the gain changes by 10, 31.6, 100 per cent respectively. The travelling wave maser is stable, probably to an even greater extent due to the built in nonreciprocity and insensitiveness to fluctuations in X'. The gain stability to load changes of a travelling wave maser is also much better than that of a cavity maser, mainly because of the dependence of gain upon the iris coupling factor in the latter.

A standard result in the theory of lossy guides is the attenuation constant α in terms of the group velocity v_g and the Q of the guide

$$\alpha = \frac{w}{Q v_g} \tag{16}$$

So defined the amplitude of the fields will decay along the circuit as $\exp(-\frac{1}{2}\alpha z)$, while the power will decay as $\exp(-\alpha z)$. In our case, however, the absorbed power is negative, the Q is negative, and we have amplification instead of attenuation. Comparing equations (11) and (16), the magnetic Q of the travelling wave maser can be defined by

$$Q_m = \frac{1}{|\chi''| F} \tag{17}$$

In discussing travelling wave maser circuits it is often convenient to define the slowing factors, and the number of free space wavelengths in the length of the structure, N, as

$$S = \frac{C}{v_g} \quad ; \quad N = \frac{\lambda}{Cf} \tag{18}$$

where C is the velocity of electro-magnetic waves in free space. The gain of the maser is then

$$G = 27.3 \frac{SN}{|Q_m|} \tag{19}$$

Part III - The Nonreciprocity Requirement

From electromagnetic theory it is known that transmission through any system is reciprocal with respect to gain or attenuation and phase unless one direction of propagation is distinguished from the other either by transport of matter or by a rotation created by a steady magnetic field. In the travelling wave tube the first is used, while in the travelling wave maser the nonreciprocity offered by the dc magnetic field is utilized through circular polarisation. The necessity for nonreciprocal propagation will now be discussed.

Consider a travelling wave maser schematically indicated in fig. 1(a). All the quantities used are defined by amplitude and phase to take into account interference due to reflections. S_{in} is the incoming signal, S_{out} the output, Γ_{in} and Γ_{out} are the reflection coefficients at the two ends and g and g^1 are the amplitude gain in the forward and reverse direction, respectively. Accounting for all reflections, the outcoming signal can be evaluated as

$$S_{out} = \frac{S_{in}\,(1-|\Gamma_{in}|^2)^{\frac{1}{2}}\;(1-|\Gamma_{out}|^2)^{\frac{1}{2}}g}{1 - gg^1\Gamma_{in}\,\Gamma_{out}} \qquad (20)$$

which suggests that the second term in the denominator if appreciable but smaller than unity will increase or decrease the amplification depending on its accidental phase. As a result, the gain will be a strongly oscillating function of frequency. If this term reaches or exceeds unity, the amplifier will oscillate.

$$\therefore \qquad |gg^1\,\Gamma_{in}\,\Gamma_{out}| \ll |$$

Similar reasoning applies to internal reflections caused by deviations from periodicity in the amplifier structure. Since reflection coefficients at the input and output smaller than 0.1 are difficult to obtain, it is

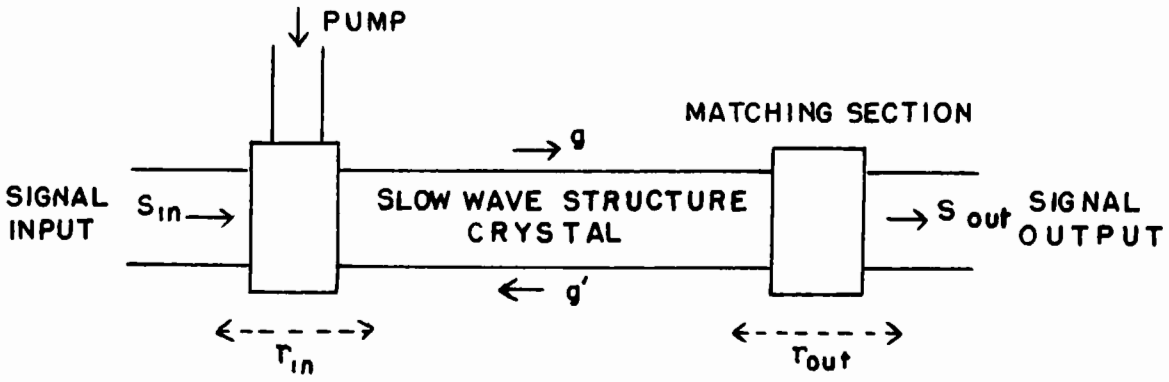

Fig. 1(a) Schematic Representation of a Travelling Wave Maser

desirable that reverse gain g^1 be much smaller than the forward gain g.

Thus the development of a unilateral travelling wave maser depends on the availability of elements exhibiting nonreciprocal attenuation. In contrast to conventional ferrite nonreciprocal devices, which operate at room temperature and at a magnetic field adjusted for optimum performance, the nonreciprocal behaviour must be achieved at a low temperature and at a field dictated by the maser operation. Two practical solutions are currently available using paramagnetic or ferrimagnetic materials.

A magnetic resonance phenomena is excited exclusively by circularly polarized radio frequency magnetic fields in a plane perpendicular to the dc field, with the sense of circular polarization determined by the direction of the applied dc magnetic field. This happens in both ferrimagnetic resonance absorption and in paramagnetic transitions. Assume that circular polarization is exhibited in certain regions of a slow-wave structure for a wave in the forward direction described by exp i(wt-kz). A wave in the reverse direction can be described by changing the sign of z or by changing the sign of t. Circular polarization implies a sequence of perpendicular field components separated by a quarter of the oscillation period. A reversal of t thus indicates a reversal of the sequence in which the field components follow one another. Hence the reverse wave is associated with the opposite sense of circular polarization. If the forward wave has strong interaction with a magnetic resonance pheonomenon by virtue of its circular polarization, the reverse wave has not and vice versa.

The first approach is to use the same paramagnetic material as that giving rise to maser gain but with an appreciably higher ion concentration. The relaxation times are then so short that the pump power employed to saturate the maser material does not appreciably affect the isolator material. Consider a structure which has distinct, separate regions exhibiting opposite

sense of circular polarization of the magnetic field. Unidirectional gain is thus obtained by placing the maser material into regions of the slow-wave structure which show, say, positive circular polarization for forward propagation. A reflected wave has negative circular polarization and does not excite the resonance. The isolator material is placed in regions exhibiting positive circular polarization for reverse propagation, (or negative polarization for the forward wave). Thus a reflected wave is absorbed by the isolator and unidirectional attenuation results. An obvious advantage in using the same crystal for amplification and attenuation is that the resonant condition for both will occur at the same magnetic field. On the other hand, a major fraction of the pump power is absorbed by the isolator.

The second method uses polycrystalline ferrimagnetic materials, such as yttrium iron garnet. These materials when placed in a region of circular polarization allow a forward wave to propagate but produce attenuation in the reverse wave due to resonant absorption. Since ferrimagnetic line widths at helium temperatures for these materials is of the order of 1000 oersteds, no care has to be taken to align the maser magnetic field with the field of the resonance isolator. Moreover the resonance absorption in ferrites is very strong compared to gain or attenuation due to paramagnetic crystals. The ferrite volume required is, therefore, small. A ferrimagnetic isolator can be expected to have lower forward loss, higher reverse attenuation and negligible pump power absorption.

It is thus necessary that the slow wave structures have certain regions of circular polarization.

SECTION II

MAGNETIC FIELDS FOR MASERS

Certain magnetic field configurations are necessary for maser operation. A dc magnetic field is essential for obtaining a Zeeman splitting of the energy levels of the paramagnetic crystal. For maser crystals the energy level separation should then be in the microwave region. The possibility of finding materials that provide the desired levels because of their internal crystalline fields remains open, but such crystals have not materialised. Most masers have been built with electromagnets, requiring well stabilized power supplies and current regulators. Recently permanent magnets have been introduced to improve the short time stability of the system, and to obtain more compact masers. For travelling wave masers the gain is dependent on the length of the structure. Large magnets are, therefore, required specially if wide bandwidths have to be attained, say, by stagger tuning. Steady magnetic fields can also be produced by solenoids. This possibility will now be discussed.

The dc magnetic field for masers must be of specified homogeneity. That is, the field should have a variation much less than the line width of the crystal resonance (a few oersted for maser crystals) in a volume equal to the crystal size[10]. This criterion does not necessarily apply to travelling wave masers, where larger bandwidths may be obtained by placing the crystal in slightly nonuniform field, i.e. stagger tuned. A preliminary analysis on solenoids showed that the field was quite uniform in the central portion, specially for large length to diameter ratios, and could be utilised for travelling wave maser applications.

To a good approximation the magnetic field at any point within the

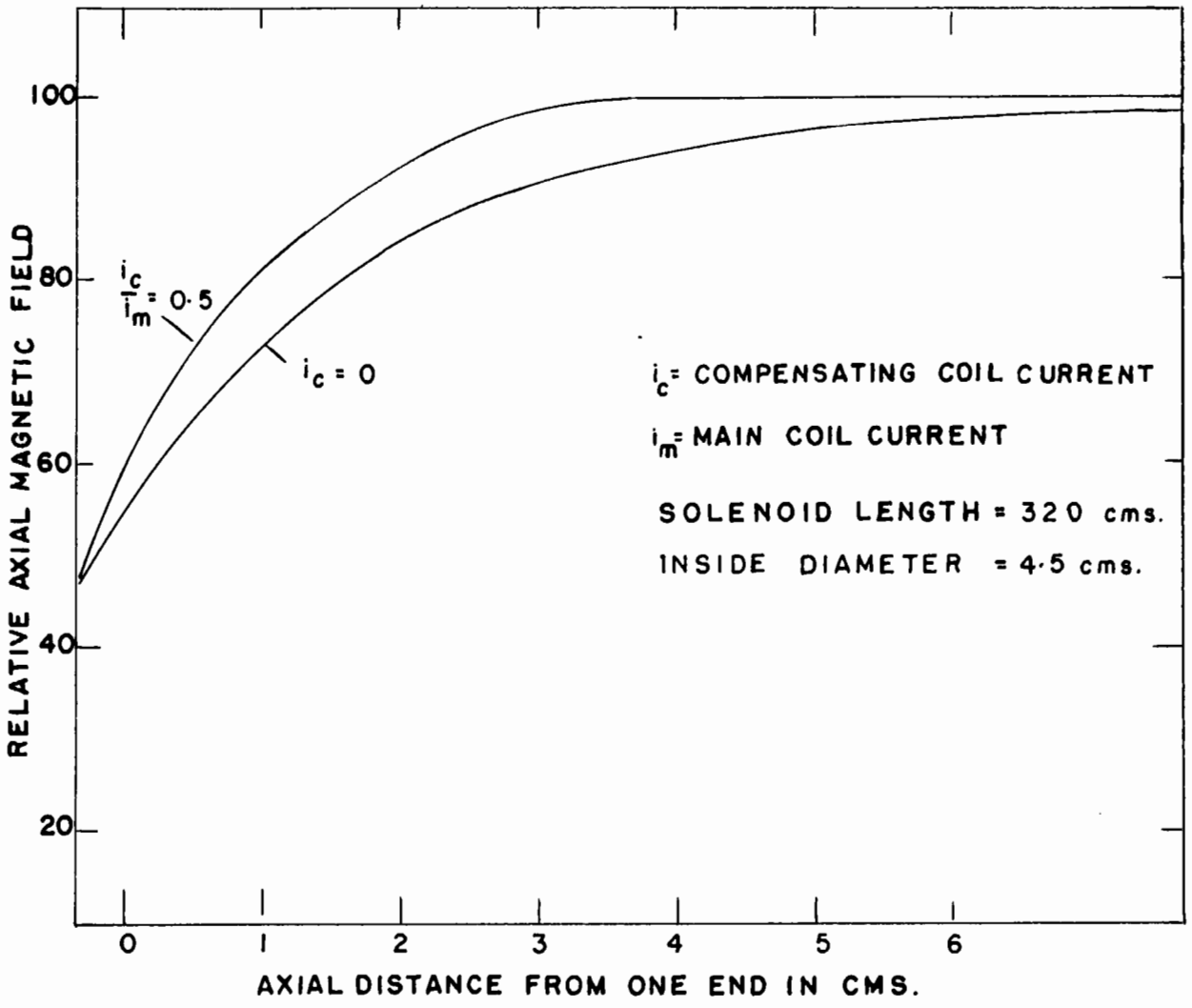

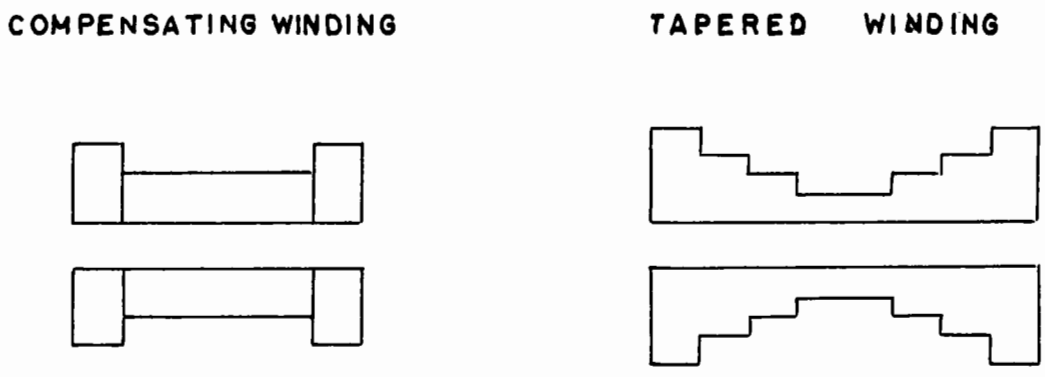

Fig. 1(b) Solenoid Field Plot

solenoid is given by

$$H = \frac{NI}{4} (\Omega_2 - \Omega_1) \qquad (21)$$

where I is the current and N the number of turns in its winding. Ω_2 and Ω_1 are the solid angles subtended by the two end cross-sections at the particular ppint. This shows a decrease in the magnetic field away from the centre, when one moves parallel to the axis and a slight increase in the field when one moves perpendicular to the axis. (The absence of a maximum or minimum is in line with the fact that there are no currents or charges present.) The field uniformity may be considerably improved by using a compensating or tapered winding, and field uniformity of 1 in 10^4 over a large volume has been obtained[15].

A solenoid designed in the Laboratory[11] had an internal diameter of 2" and a length of 14". The solenoid used a compensating winding and the magnetic field plot is shown in fig. 1(b). For maser work a diameter of at least 3" is required so that a refrigerating dewar may be inserted. To obtain the same homogeneity as in the above example, a longer solenoid would be necessary. It is roughly estimated that a 20" solenoid would provide a 5" operating length around the centre of the solenoid.

Fields up to a 1000 oersted are often sufficient for maser work. The solenoid mentioned above produced fields greater than 200 oersted/ampere. To obtain a well stabilized magnetic field current regulators are required. Since it is difficult to regulate large currents, high magnetic fields are not easily obtainable.

The application of solenoids is especially interesting due to the recent operation of superconducting magnets and solenoids[16]. The solenoid and magnet coils, made out of niobium (Nb) wire (superconducting below 8.5°K),

are limited to fields below approximately 2000 oersted (dependent on strain in metal, impurities and temperature). Higher fields can be obtained by using a compound of niobium and tin, but drawing a wire out of this compound is relatively difficult. A superconducting solenoid can very easily be placed in a dewar, doing away with massive magnets, power supplies and current regulators. The solenoid, placed in a constant temperature liquid the bath will also produce a magnetic field of high stability.

If solenoids are used, the magnetic field would lie in the direction of propagation, and field configurations would be different from travelling wave masers operated so far. Since the wave has to be circularly polarized to produce nonreciprocal gain, the slow-wave structure would be required to show circular polarization in a plane normal to the direction of propagation. This dissertation discusses various slow-wave structures which may be used in conjunction with solenoids. With slight modifications, some of the structures can also be used with magnets.

SECTION III

SLOW WAVE STRUCTURES

There are three methods of producing slowing of an electromagnetic wave: dielectric, geometric and resonant.

Dielectric slowing: It is well known that the speed of a wave is reduced in dielectric media, given by $\sqrt{\mu/\epsilon}$. The slowing factor is approximately equal to $\sqrt{\epsilon}$. Most materials with a high dielectric constant are lossy, temperature sensitive and unstable. Although this method is not directly used, the paramagnetic crystal itself produces slowing.

Geometric slowing: Slowing may be obtained by modifying the centre conductor, of a coaxial system, into the form of a helix or meander line. Propagation may then be crudely described by a TEM wave propagating along the line with velocity of light and producing a slower effective group velocity in the direction of propagation. It is difficult to obtain a slowing factor greater than 100 by this method. Theoretically such a structure should propagate at all frequencies. However, at high frequencies, depending on the pitch, the successive conductors couple to each other resulting in periodic structure type behaviour and a dispersion characteristic. A disadvantage of such structures is that the fields drop off exceedingly fast, allowing energy to interact with few spins. The conventional helix has a drawback in that the rf field spirals around with the line. A possible solution is a flat helix discussed by DeGrasse et al., but the slowing factor obtained is small.

Resonant slowing: The resonant type of slow wave structure consists of a periodic array of resonant circuits coupled in some fashion to their neighbours. The theory of periodic structures has been extensively dealt with in literature[8]. Certain properties relevant to travelling wave maser circuits will be considered here.

The basis for a study of periodic transmission systems is a theorem due to Floquet. For a given mode of propagation, at a given frequency, the fields at one cross-section differ from those one period away by a complex constant. This is evident if the whole structure is displaced along its length by one period, L: It coincides with the original structure, so that new fields can differ from the first one only by a constant factor. A general constant fulfilling these conditions is $e^{-(\gamma+2\pi n\, j/L)z}$. It can be shown analytically that for periodically loaded systems γ is either real or pure imaginary leading to attenuation and pass bands respectively. In pass bands a Brillonin zone type dispersion characteristic (frequency-phase) exists. In a pass band $\gamma = j\beta_o$ (say) and we may write

$$\beta_n = \beta_o + \frac{2\pi n}{L} \tag{22}$$

where n is a positive or negative integer and β_o the phase shift per unit length. This reveals the following characteristics in periodic transmission systems:

1. There exist certain pass and stop bands. Certain frequencies can propagate down the structure with little or no attenuation whereas other frequencies are attenuated at a rapid rate. These frequencies occur in bands.

2. The fields can be analysed in a Fourier series with infinite number of components. The disturbance can be regarded as a superposition of an infinite number of travelling waves. The fields are of the form

$$E(x, y, z)e^{jwt} = \sum_{n=-\infty}^{\infty} E_n(x, y)e^{jwt}\, e^{-j\beta_n z} \tag{23}$$

3. There is no unique phase velocity, v_p. At any frequency, for a given mode of propagation, each component has a different v_p, given by w/β_n and a wavelength $2\pi/\beta_n$. These components are therefore called space harmonics. The space harmonics have the same group velocity, v_g, given by

$$v_g = \frac{dw}{d\beta_n} = \frac{dw}{d(\beta_o + \frac{2\pi n}{L})} = \frac{dw}{d\beta_o} \qquad (24)$$

Thus the electromagnetic energy is transmitted without division by the group of space harmonics as a whole. The harmonics are all necessary and cannot be separately excited. The amplitude of the harmonics, E_n, depends on the unit cell of the structure, and except for complicated structures it is the fundamental ($n = 0$) component which has the largest amplitude.

4. The phase velocity for any point on the dispersion curve is given by the slope of the line joining the point to the origin. The group velocity is given by the slope of the curve at the particular point. The group velocity goes to zero at the ends of the pass bands. There is then no propagation of energy and attenuation bands take over. In practical circuits there is no sharp cutoff so that operation in the cutoff region is possible.

The group velocity is given in terms of the phase velocity by

$$v_g = v_p \left(1 - \frac{w}{v_p} \frac{dv_p}{dw}\right)^{-1} \qquad (25)$$

We see that the group velocity may be much smaller than the phase velocity if $-\frac{dv_p}{dw}$ is large. As a result, various periodic structures which are very narrow band for travelling wave tube applications will have wide travelling wave maser bandwidths.

In masers it is really the energy velocity we are interested in. However, the energy velocity is equal to the group velocity so long as absorption and attenuation of the wave are small[9]. From equation (16) we note that low group velocities lead to high attenuation. Hence near cutoff the attenuation is high and group velocity ceases to have a clear physical meaning, but the energy velocity can still be defined. The energy flow gives the energy passing from cell n to cell (n + 1) per unit time. The energy velocity

is defined as the energy flow divided by the energy density and gives the rate at which energy flows along the structure. Here we shall consider only the central portion of the dispersion characteristic because, although high slowing can be obtained near cutoff the variation in slowing is large, leading to small maser bandwidths. Moreover it is difficult to couple into a structure operating near the cutoff frequency. Thus for our purposes the group velocity is equal to the energy velocity and equation (6) follows.

The group and phase velocities are parameters which are often easily controllable without much affecting the stored energy per unit length. For instance, in resonators coupled by loops and irises, the stored energy is not much affected by the loops or irises unless they are very large, but v_p and v_g are greatly changed by small changes in coupling.

A basic procedure for finding the $w - \beta_o$ diagrams for coupled resonator structures is as follows: a slight amount of coupling is introduced into an array of originally uncoupled resonators and the effect on the two cutoff points is investigated. Another method is to start with a homogeneous transmission line and determine the change on introduction of a slight amount of loading. The first method will be taken up here since it shows how the group velocity can be varied.

The change in the two cutoff frequencies (for $\beta_o L = 0$ and $\beta_o L = \pi$) due to a change in coupling, depends on how the field lines have changed. If the electric field is perturbed the cutoff frequency will increase, while a magnetic field perturbation causes a decrease in frequency. Inductive and capacitive coupling can be defined as coupling schemes where H and E lines respectively link the resonators.

Consider an array of rectangular uncoupled resonators placed end to end, resonating in the TE_{10} mode. Figure 2 shows such a structure having field lines drawn in for the two cutoff points $\beta_o L = 0$ and $\beta_o L = \pi$.

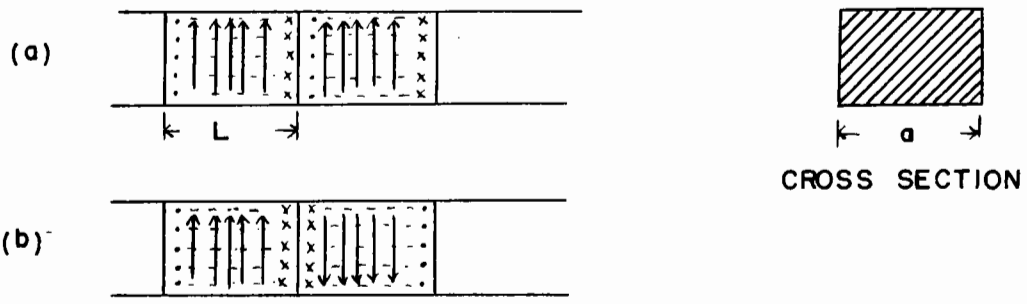

Fig. 2 Rectangular waveguide with periodic partitions.
(a) Field pattern for $\beta_o L = 0$ (b) Field pattern for $\beta_o L = \pi$
Solid lines = E field; Dashed lines = H field.

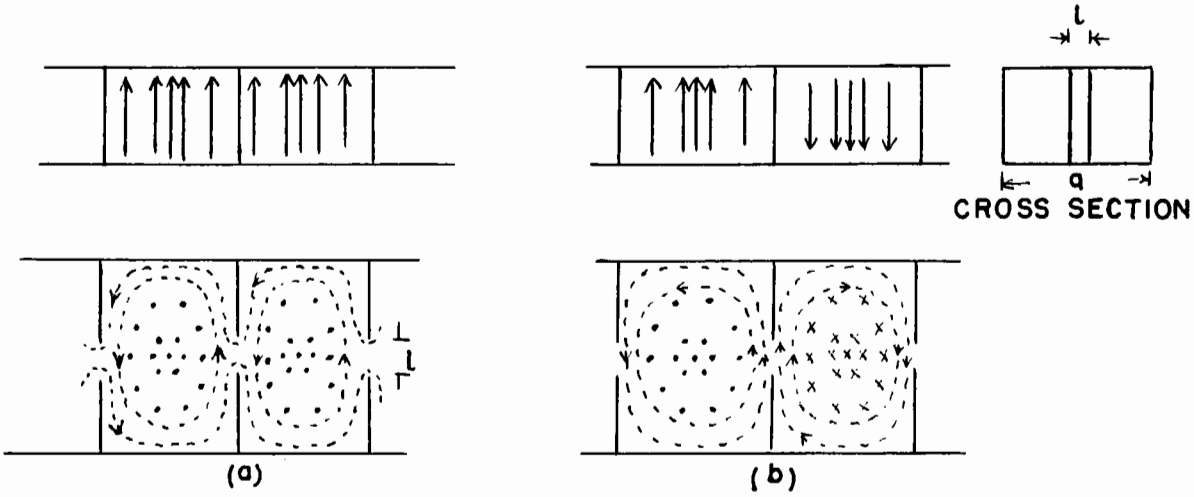

Fig. 3 Pure inductive coupling. Field patterns (a) $\beta_o L = 0$; (b) $\beta_o L = \pi$

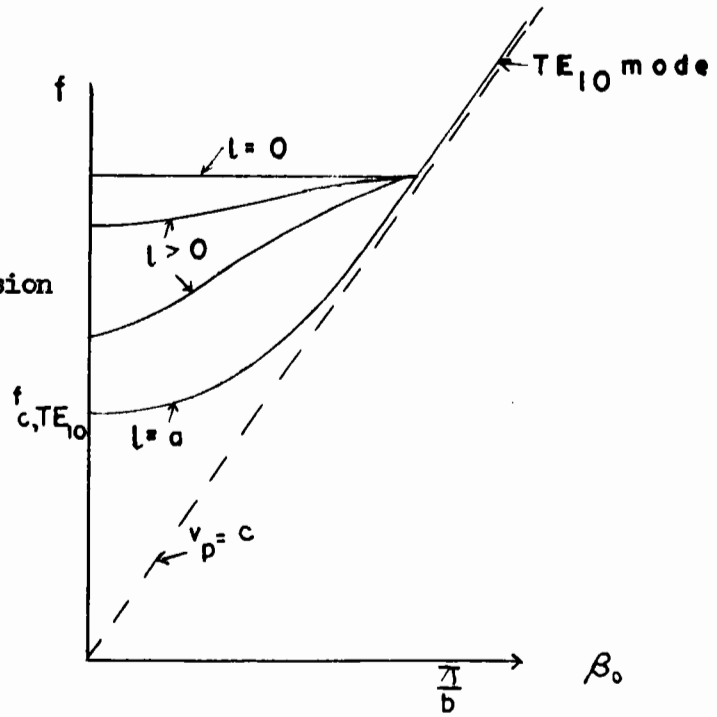

Fig. 4 Dispersion Curves

The resonance frequency for both these points is the same. When a small vertical slot is cut in the thin partitions, as shown in fig. 3, a certain amount of inductive coupling is introduced. The field configuration for $\beta_o L = \pi$ is unchanged and so is the resonant frequency. For $\beta_o L = 0$ however, the H lines link the cavities causing inductive coupling and a decrease in the resonant frequency. The change in $w - \beta$ diagram is shown in fig. 4.

In fig. 5, the resonators are placed top to top. When a small hole is cut in the centre of the thin partition E lines penetrate into the adjoining cavity leading to pure capacitive coupling. The E lines are not affected for the point $\beta_o L = 0$ (in fig. 6a) but are strongly perturbed for $\beta_o L = \pi$ and hence an increase in the higher cutoff frequency. When all partitions are removed, the propagation characteristic becomes that of the TE_{11} mode, as shown in fig. 7. Mixed coupling is characterized by the presence of both E_z and H_z lines in the coupling aperture, and these often produce opposite affects. For example, consider the case of pure capacitive coupling (fig. 6). If in addition to the capacitive coupling hole a slot is cut on the periphery of the partition wall as shown in fig. 8, a combination of capacitive and inductive coupling is achieved. It will be noted that the slot introduces perturbations in the magnetic field, does not affect the $\beta_o L = 0$ cutoff, but lowers the $\beta_o L = \pi$ cutoff frequency. Thus the addition of an inductive slot decreases the originally capacitive passband. Proper adjustment may reduce the passband to the resonant frequency of uncoupled resonators which means the net coupling is zero. When the inductive component is dominant, a backward wave is propagated, i.e. the group and phase velocity are of opposite sign.

The propagation along a structure consisting of an array of resonators can thus be controlled by adjusting the coupling. When the net coupling is zero, the $w - \beta_o$ characteristic is a straightline, group velocity is zero

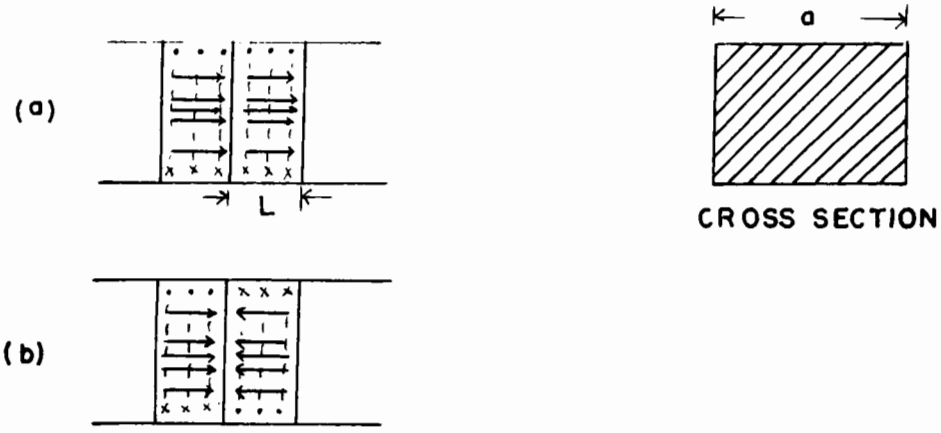

Fig. 5 Rectangular TE_{101} resonators with top surfaces against each other. (a) $\beta_o L = 0$; (b) $\beta_o L = \pi$

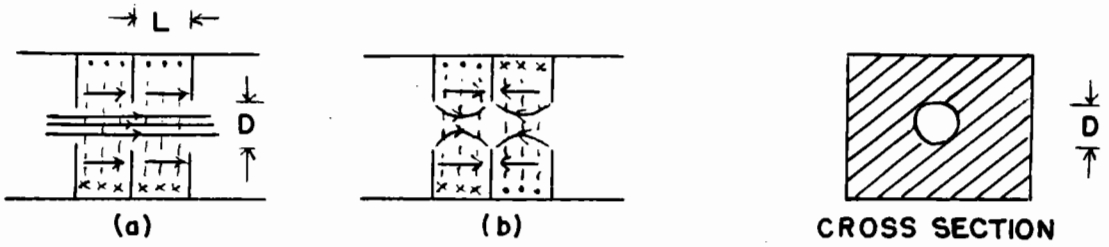

Fig. 6 Pure capacitive coupling. Field patterns
(a) $\beta_o L = 0$ (b) $\beta_o L = \pi$

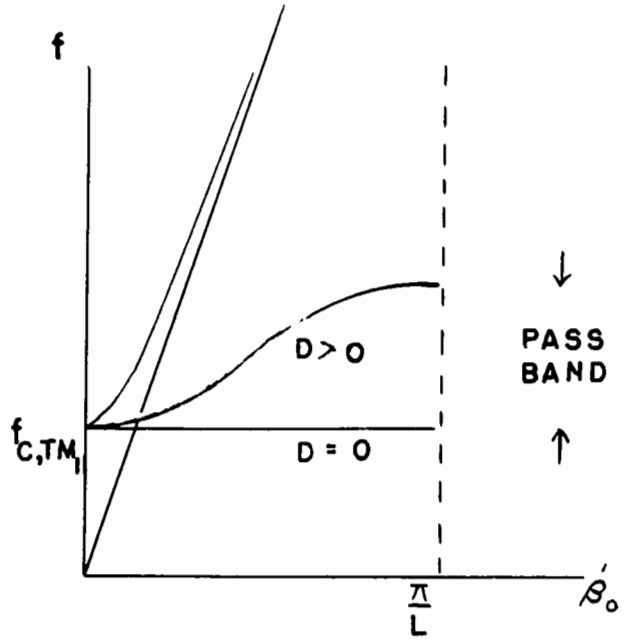

Fig. 7 Dispersion Characteristic

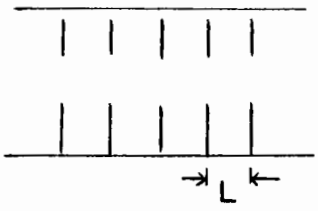

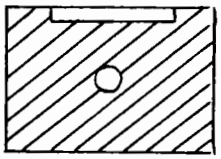

CROSS SECTION

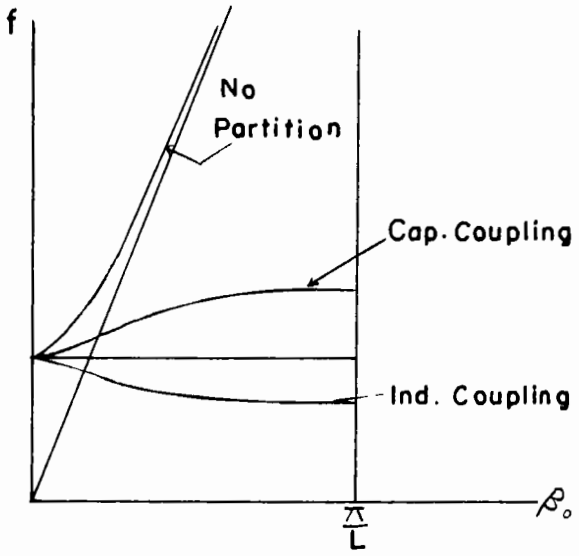

Fig. 8 Mixed coupling and Dispersion Curves

and the structure does not propagate. On introduction of a slight amount of coupling a finite bandwidth is obtained and propagation occurs. The shape of the $w - \beta_o$ curve, i.e. the slope, and hence the group velocity are thus dependent on the coupling. A small v_g and therefore a high slowing factor is obtained for small coupling. Thus, in general, the narrower the structure passband the higher is the slowing.

Periodic slow wave structures for wideband amplifiers may briefly be divided into two classes, waveguide structures and line structures. The first is significant due to the various possible modes of propagation and in the absence of a TEM mode. Periodic obstructions split each mode into alternate pass and stop bands. In general the different modes of the guide get mixed up with each other, so that a very complicated situation exists for higher frequencies. Such structures have been widely used in travelling wave tubes and linear accelerators, but have not found application in masers. Certain possibilities will be considered in the next section. Line structures, such as the interdigital line and easitron used in travelling wave tubes and comb structures used in travelling wave masers are open structures, requiring neither a ground plane nor a shielding enclosure. Both classes of structures may be described as coupled resonator structures, but in line structures the coupling is not necessarily limited to the nearest neighbours.

One family of line structures, the ladder line, consists of an array of parallel wires transverse to the direction of propagation and terminated in various fashions. These structures were a natural choice for travelling wave masers, for they had the great advantage of having distinct regions of circular polarization of the magnetic field. The plane of circular polarization is normal to the length of the wires, as will be shown in the next section. The dc magnetic field applied must thus be along the wires. These structures may hence be placed as such between the poles of a magnet. However, to be

used with solenoids, they require modification. The structures can be modified by skewing, as shown in fig. 14. They can then be 'wrapped' in the form of a spiral and placed along the axis of a solenoid. The wires are then essentially in the direction of propagation. If placed symmetrically inside a solenoid the wires will all be at the same distance from the axis. It will be noted that by this means a longer structure can be incorporated and a combination of resonant and geometrical slowing should result.

In this research program special emphasis was laid on low microwave frequency structures, most of the measurements being in the L band. A low noise travelling wave maser would be particularly useful for the measurement of weak cosmic radiation, particularly for the line near 1420 Mc/s emitted by interstellar atomic hydrogen. At these frequencies structures tend to be quite large and various possibilities are examined for reducing the size of the structures for a compact travelling wave maser.

SECTION IV

STRUCTURES FOR TRAVELLING WAVE MASERS

Part I - Waveguide structures

Waveguide structures have so far not been used in travelling wave masers. The serious drawback arises from the fact that the structure has to propagate the signal as well as the pump frequency. Both frequencies must therefore lie in one of the pass bands of the structure. Since the higher pass bands in waveguide structures tend to be narrow, the two frequencies cannot be much different. However, for sufficient inversion it is advantageous to have $f_{pump} \gg f_{signal}$. The above difficulty adds a further restriction on the operation of a travelling wave maser.

These structures, however, may be used in resonance studies where only the signal frequency is propagated. The bandwidth of the guide may be increased by the addition of ridges. With ridges an X-band waveguide can propagate frequencies from 4 to 15 Kmc/sec. Since a circularly polarized wave is required, a preference for transverse magnetic modes is indicated. The cross-section of the guide is also required to be symmetrical requiring quadruple ridges. Cylindrical or square waveguides can be used. Field solutions of quadruple ridge waveguides have not been worked out, but the cutoff frequency can be obtained from an equivalent circuit and the field configurations can be approximated from rectangular and circular waveguide configurations. Periodicity may be obtained by introducing irises or by cutting slots in the ridges.

Part II - Ladder line structures

In recent years slow wave structures consisting essentially of arrays of parallel conductors have become of increasing importance because of their use in travelling wave devices. The first structure of this family was the easitron structure, first considered by Walker. The structure consisted of closely spaced thin parallel wires, extending between and normal to two infinite parallel perfectly conducting planes. One wire acts as a resonator, having natural frequencies at which it is an integral number of half wavelengths long. It can support a variety of TEM waves with the field normal to the wires, each one corresponding to a different mode of excitation of the wires. The relevant case is that in which there is simply a phase change βL from one wire to the next. Whatever the value of β, the short circuited array can support TEM standing waves at the frequency for which the free space wavelength λ is twice the length of the wires, i.e. the first resonant frequency. In circuit terms the wires are uncoupled and it can be shown that the magnetic and electric couplings are equal and opposite. The dispersion curve is a horizontal straight line, the group velocity is zero and the structure does not propagate.

Several characteristics of the easitron structure can be noticed (see fig. 11a). The field vectors are everywhere parallel to the shorting planes. The electric vector E is an even function of $y - \frac{h}{2}$, having a maximum amplitude at $y = \frac{h}{2}$ and vanishing at the planes. The magnetic vector H is an odd function of $y - \frac{h}{2}$, having a maximum amplitude at the planes and vanishing at $y = \frac{h}{2}$. Thus the vertical plane of symmetry $y = \frac{h}{2}$ is an equipotential plane for the slow wave structure. If the structure is cut into half along this plane, two identical 'comb' structures result. The characteristics of the comb structure are similar to that of the easitron. The length of the wires now corresponds to $\lambda/4$. The magnetic and electric field

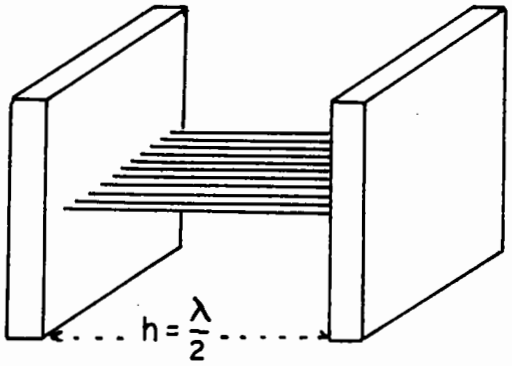

(a) EASITRON STRUCTURE

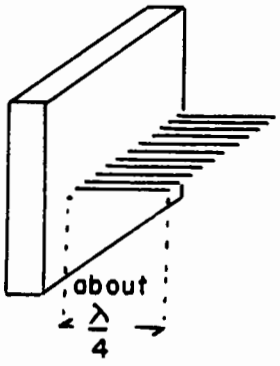

(b) COMB STRUCTURE

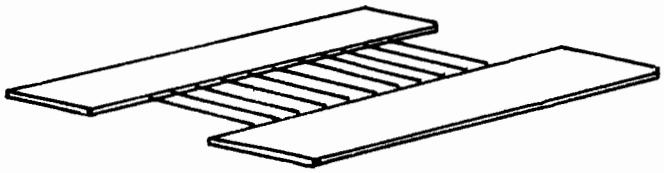

(c) PROPAGATING LADDER LINE

An array of wires bridging a gap between two planes forms a slow wave structure.

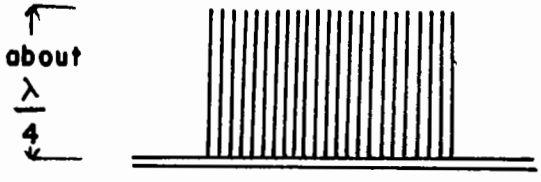

(d) PROPAGATING COMB STRUCTURE

An array of wires shorted at one end by a wire

Fig. 10 Various Ladder Structures

couplings are still equal and opposite and no propagation results. But the energy stored is roughly half the stored energy of the easitron.

The easitron may be enclosed in a rectangular waveguide. The two side plates merely form two extra conductors in the multi-conductor transmission line. The dispersion curve is absolutely unaltered, but the field distribution is modified when the horizontal plates are very close to the ladder. The structure may be made to propagate by upsetting the equality of the inductive and capacitive coupling. Walker used the easitron in a tube by distorting the wires. Karp found that if the array of wires extends across a slot cut in a conducting plane as in fig. 10(c) or across a channel milled in a conducting block, the wires are somewhat coupled and the structure forms a circuit which will sustain progressive waves. This coupling comes about because the fields, and particularly the magnetic field near the ends of the wires, is a little different from the fields for wires between parallel planes, and so the electric and magnetic coupling do not cancel. A distortion of the waveguide enclosing the ladder structure also brings about propagation. The Karp propagating structure can be obtained if one or two central ridges are added. This increases the electric field coupling between the wires. Propagation can also be obtained in the waveguide case by pushing in ridges at the sides of the shorting plates where the electric field is weak and the magnetic field is strong. The magnetic coupling is then greater than the electric coupling, and a backward wave is propagated. Some structures along with their dispersion curves are shown in fig. 11.

Comb structures (fig. 10b) have been used with considerable success in travelling wave masers. The array of combs is enclosed in a waveguide and propagation obtained by introducing electric field perturbation. Thus capacitive coupling predominates and a forward wave is propagated. A typical maser comb structure is shown in fig. 12(a), which also shows the maser

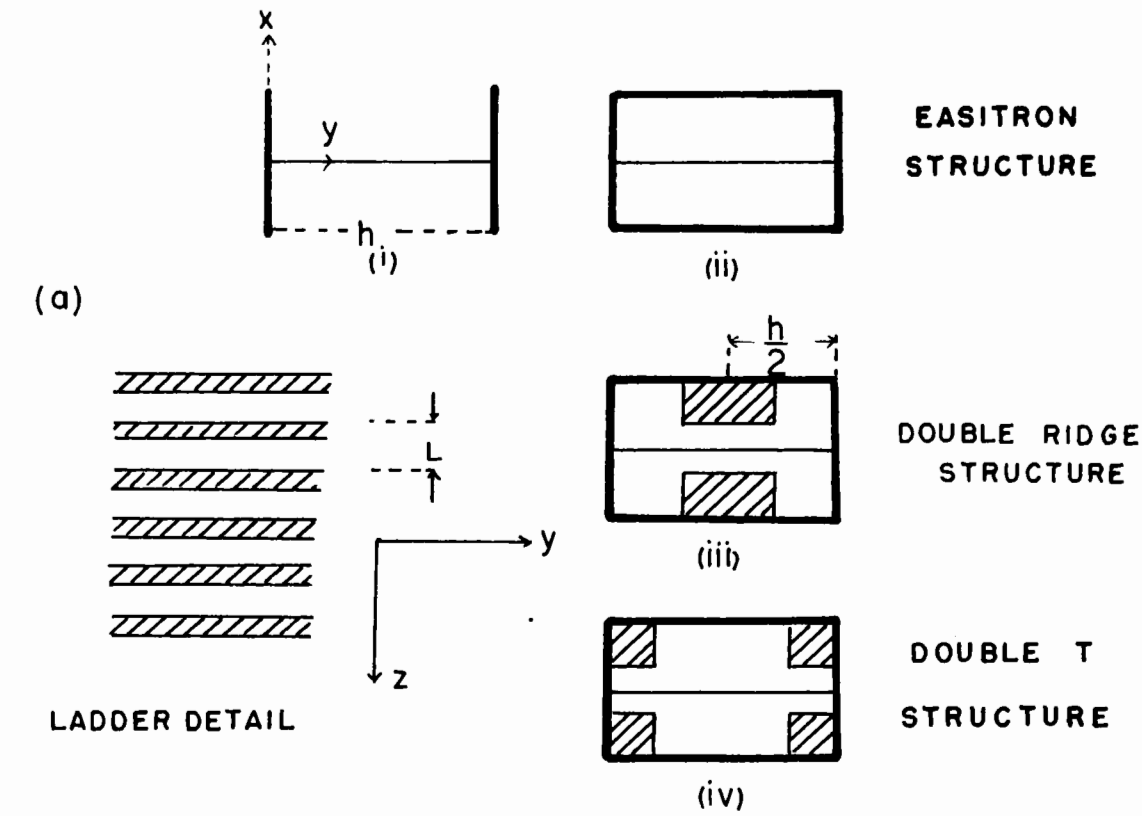

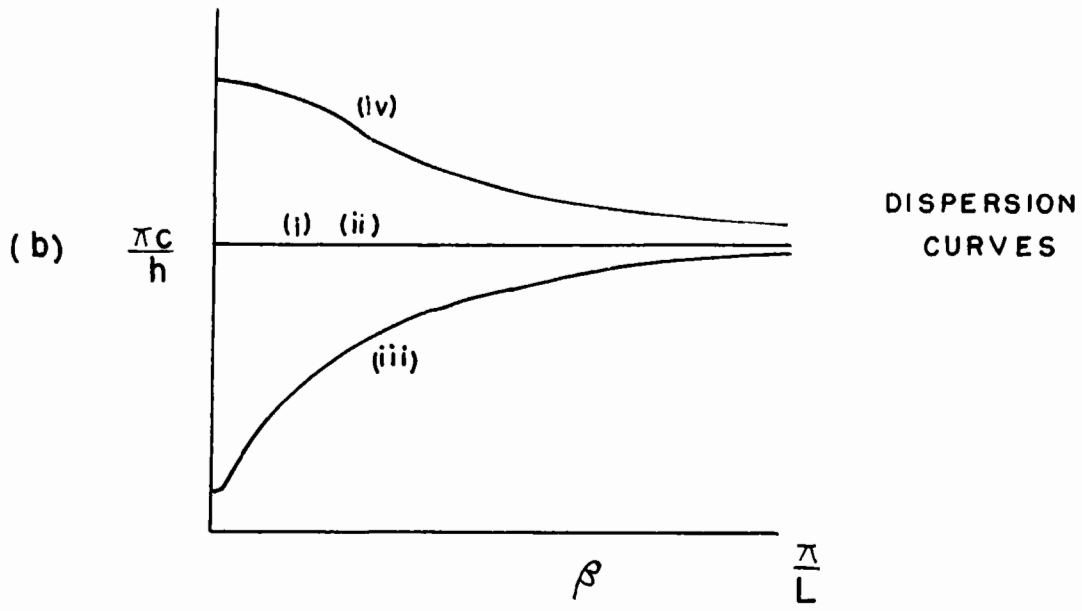

Fig. 11 Propagation along Ladder lines

crystal and isolator in position. The field configurations for such a structure are also shown. The comb structure will now be considered in detail.

Part III - Comb structures

The pure comb consists of an array of identical parallel fingers, short circuited at one end and open circuited at the other. The pure comb will not transmit electromagnetic energy along its length. If a finger is excited the wave bounces back and forth between the open and short circuited ends; it is not passed on to the adjacent fingers as the net coupling between fingers is zero. The group velocity is zero for a pure comb. By introducing a small perturbation like a capacitive coupling, a connecting link between the fingers is provided to propagate a signal along the comb. The capacitive coupling can be provided at the open ends either by a capacitive loading plate or by loading the individual fingers. The bandwidth and group velocity can be varied by varying this coupling. It may be mentioned here that loading the ends of the fingers decreases the resonance frequency, due to increased end effects.

When a pure comb is excited at the signal frequency, a standing wave is set up on each finger consisting of two waves travelling along it in opposite directions, with the velocity of light. Since the finger tip is open circuited, the current along it varies like $\sin(2\pi y/\lambda)$ where λ is the free space wavelength. Since at the base there is a short circuit, i.e. a current maximum,

$$\frac{2\pi h}{\lambda} = \frac{\pi}{2} \qquad \text{and} \qquad h = \frac{\lambda}{4} \tag{26}$$

This neglects any end effects, and shows the infinitesimal pass band for an ideal comb.

The magnetic field distribution is hardly disturbed by the capacitive loading and is the same as in fig. 13. Since the current flows along the fingers, the magnetic field encircles the fingers and the electric field points radially from them. Hence both fields are in the x-y plane.

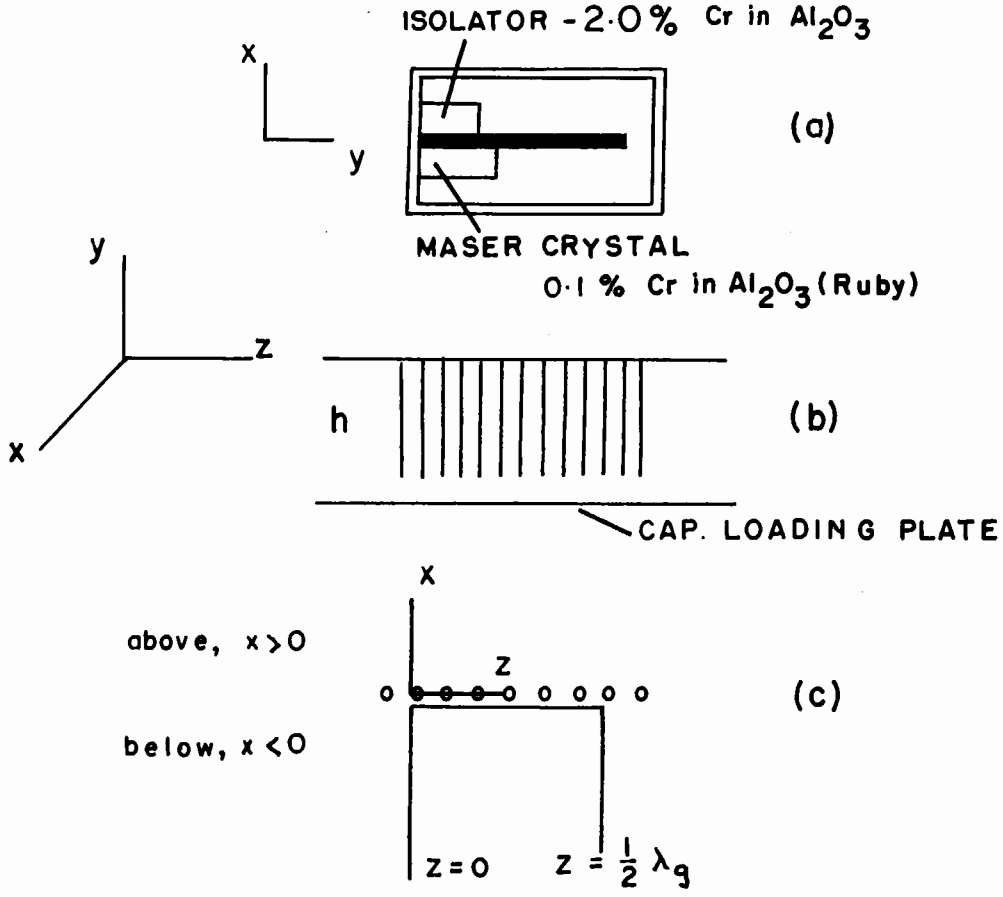

Fig. 12 (a) Typical Maser cross section (b) Side view (c) Top view

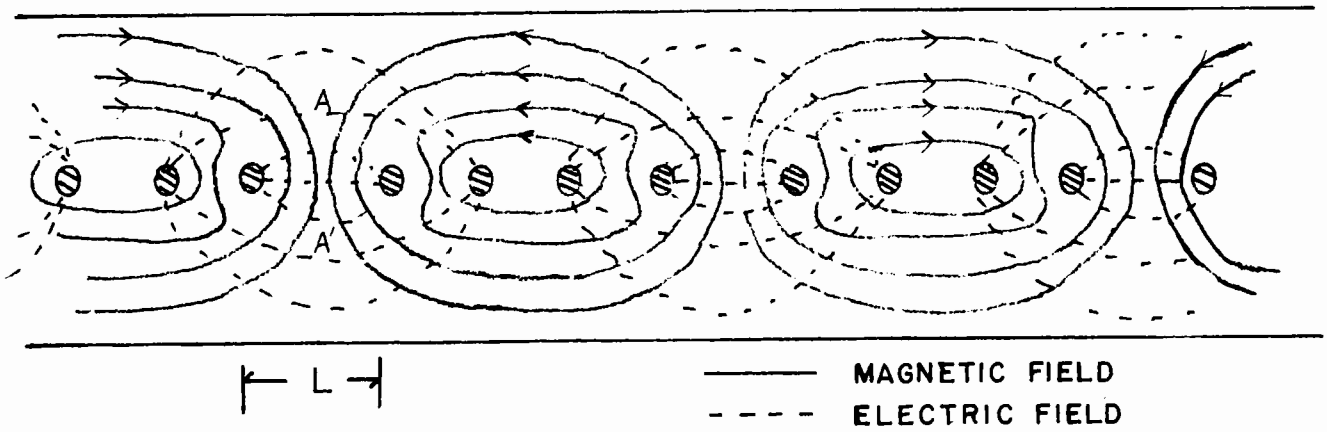

Fig. 13 Field configuration for a phase difference of $\pm \frac{\pi}{4}$ between the fingers (one period)

The essential properties of the magnetic field distribution can be obtained by recognising that the primary function of the fingers is to prevent conduction in the z-direction. An approximation usually made for structures of this type is to consider that the comb behaves like a smooth sheet which conducts perfectly in the y-direction and does not conduct at all in the z-direction. To this degree of approximation the comb is uniform in the z-direction and the field depends on z through a factor $\exp(-j2\pi z/\lambda_g)$. The magnetic field depends on y through the same factor as the current along the fingers: $\sin(2\pi y/\lambda)$. Finally, since the field must fall to zero away from the comb, it must depend on x through a factor $\exp(\Gamma x)$ where Γ is the attenuation coefficient in the negative x-direction (i.e. below the combs). Hence apart from an amplitude factor we have

$$H_x = \sin(2\pi y/\lambda) \exp\left[\Gamma x - j\, 2\pi z/\lambda_g\right] \qquad (27)$$

$$H_z = B \sin(2\pi y/\lambda) \exp\left[\Gamma x - j\, 2\pi z/\lambda_g\right] \qquad (28)$$

where B is a constant determined by Hz/Hx. The field components satisfy the wave equation

$$\frac{d^2U}{dx^2} + \frac{d^2U}{dy^2} + \frac{d^2U}{dz^2} + \left(\frac{2\pi}{\lambda}\right)^2 U = 0$$

Substituting values for H_x and H_z for U we have

$$\Gamma = \frac{2\pi}{\lambda_g} \qquad (29)$$

i.e. the attenuation coefficient away from the guiding structure is equal to the phase change coefficient in the direction of propagation.

Ampere's law is used to evaluate the constant, B: the line integral of the magnetic field round any closed path is equal to the current threaded through it. The rectangular path in the x-z plane (see fig. 12c), which is

closed at infinity, has no current threaded through it; no conduction current because it is in free space and no displacement current because Ey = 0. Hence

$$\int_{-\infty}^{0} H_x(x, y, 0)dx + \int_{0}^{\lambda_g/2} H_z(0, y, z)dz + \int_{0}^{-\infty} H_x(x, y, \tfrac{1}{2}\lambda_g) = 0$$

or
$$\text{Sin}\left(\frac{2\pi y}{\lambda}\right)\left[\frac{\lambda_g}{2\pi} + B\frac{\lambda_g}{j\pi} + \frac{\lambda_g}{2\pi}\right] = 0 \qquad (30)$$

whence $B = -j$

Thus the magnetic field distribution below the comb is

$$H_x = \sin\left(\frac{2\pi y}{\lambda}\right) \exp\left[2\pi(x-jz)/\lambda_g\right] \qquad (31)$$

$$H_z = -jH_x \qquad (32)$$

For the magnetic field above the comb ($x > o$ and $\exp(-\Gamma x)$) we get $H_z = jH_x$. Thus the magnetic field is circularly polarized, above and below the comb, with an opposite sense of rotation.

If the shorting plane of the comb structure is replaced by a rod (fig. 10d), the structure propagates, probably because the magnetic coupling has been reduced. We are currently interested in structures of this type some examples of which are shown in fig. 14. These are all open structures[5], and do not require ground planes. (This may be of advantage in optical pumping systems.) All structures in fig. 14 are bandpass structures, except the ungrounded comb which is a low pass structure. The grounded comb is the most promising of these structures. The skewed comb structure is a little different from the rest. Variable magnetic field coupling may be obtained by changing the slant angle. This skewed structure is of particular interest because it can be 'wrapped' in the form of a spiral for use with a magnetic field produced by a solenoid.

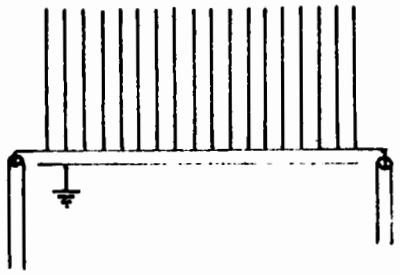

(a) UNGROUNDED COMB

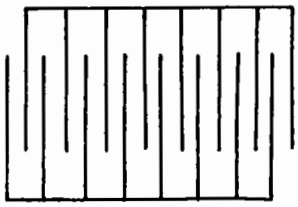

(b) INTERDIGITAL LINE

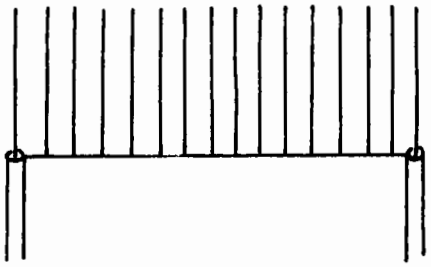

(c) GROUNDED COMB

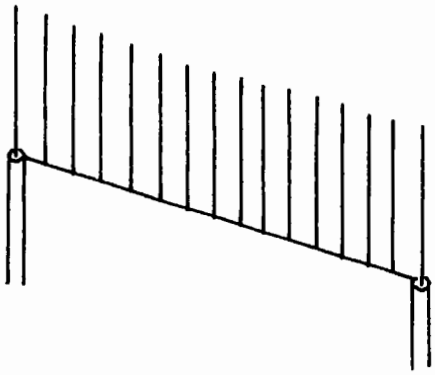

(d) SKEWED COMB

Fig. 14 Various Comb Structures

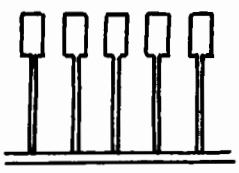

Fig. 15 Loaded Comb Structures

At low microwave frequencies the combs tend to become quite large. The length of the combs, for a certain frequency range, can be reduced by dielectric loading or by loading and distorting the ends of the fingers. The ends may be loaded as shown in fig. 15. This method increases the end effects with the result that the electrical length of the fingers is much greater than h. The magnetic field configuration is hardly changed by these modifications. However there is a corresponding change in the pass band and group velocity due to increased capacitive coupling.

Part IV - Theory of propagation along slow wave structures consisting of arrays of parallel conductors

Precise theoretical analysis of these structures by means of field matching techniques presents formidable difficulties. Certain assumptions have to be made to simplify the analysis. One assumption generally made is that the field distribution in such structures may be represented by a TEM wave or a sum of such waves propagating in the direction of the conductors. This method was first used by Fletcher and applied to an interdigital line. Hiw analysis contained an algebraic error, which was corrected by Walling[13]. Leblond and Mourier[14] also analysed such structures assuming a quasi-electrostatic field distribution in the (x-z) plane. They neglected coupling between non adjacent neighbours and the evaluation of their result required the experimental determination of the capacitance between different parts of the circuit. Following on the lines of Fletcher's treatment, certain characteristics of comb structures are derived here. The method of analysis has the following basic assumptions:

(1) The structure can propagate a EM wave in the direction transverse to the array of parallel conductors forming it, the voltage on m^{th} conductor is then given by

$$V_m = V_o \exp\ j(wt - m\theta) \qquad (33)$$

where $\theta = \beta L$ is the phase shift per period L.

(2) The field distribution around the structure can be represented by a TEM wave or a sum of such waves propagating in the direction of the conductors. The number of TEM waves required to describe the propagation is determined by the periodicity of the boundary conditions. If the boundary conditions are repeated for every N^{th} conductor N waves are required. Thus one TEM wave describes a comb structure.

These two assumptions are inconsistent since (1) implies an energy flow normal to the conductors whereas assumption (2) provides no field components to maintain such a flow. The Poynting vector in the z-direction is zero because there is no electric or magnetic field in the y-direction. The field components which provide the transverse energy flow in an actual structure of this type occur at discontinuities in the array of conductors i.e. finger ends in comb structures, edge of ridge in a Karp structure. Thus the second assumption will be valid provided that the energy stored in the discontinuity region is much less than that stored in the regions where the field distribution can accurately be represented by TEM waves. In general the analysis is valid provided the length of the conductors forming the array is much greater than the separation of successive conductors.

The most important factor in this TEM wave treatment is the characteristic admittance of a single conductor in the array. The voltage on successive conductors in a given plane are related by equation (33). The characteristic admittance of a single conductor in this array may then be defined by

$$Y(\theta) = \frac{I_m}{V_m} \tag{34}$$

For rectangular conductors $Y(\theta)$ is given by (see Appendix III)

$$Y(\theta) = \sqrt{\frac{\epsilon}{\mu}} \left[\frac{4d}{\ell} \sin^2\left(\frac{\theta}{2}\right) + 4 \frac{L-\ell}{L} \sin\left(\frac{\theta}{2}\right) S(\alpha) \right] \tag{35}$$

where $\alpha = \ell/L$ and

$$S(\alpha) = \sum_{n=-\infty}^{\infty} (-1)^n \left[\frac{\sin(\theta+2\pi n)\frac{\ell}{2L}}{(\theta+2\pi n)\ell/2L} \right] \left[\frac{\sin(\theta+2\pi n)\frac{L-\ell}{2L}}{(\theta+2\pi n)\frac{L-\ell}{2L}} \right] \tag{36}$$

If the boundary conditions are repeated for every Nth conductor N waves are required having phase constants

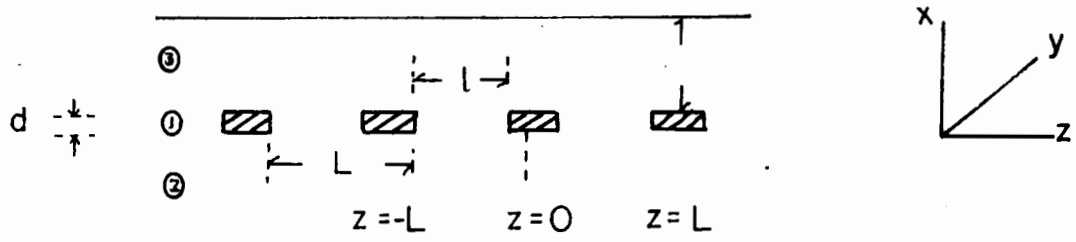

(a)

Cross section of schematic ladder line circuit with rectangular fingers

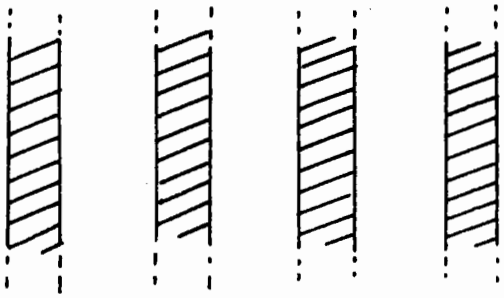

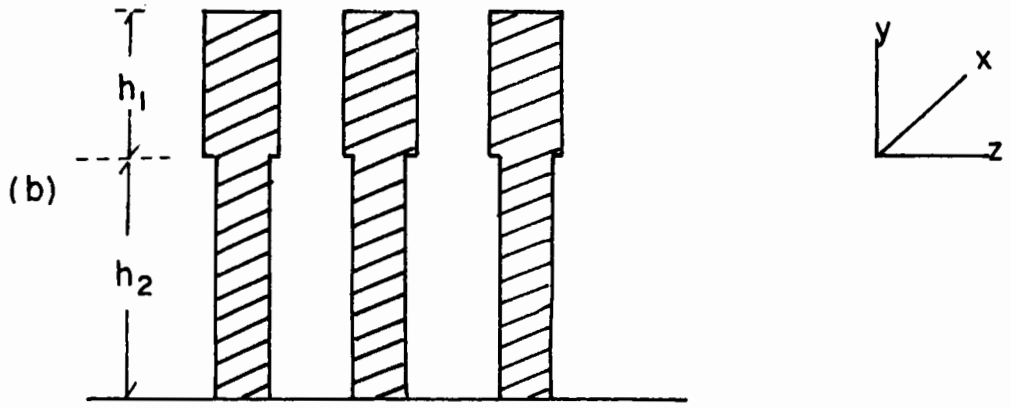

(b)

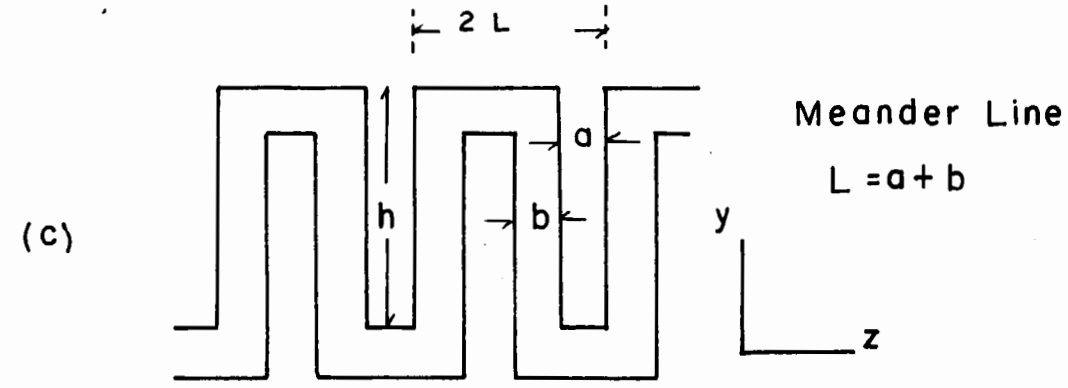

(c)

Fig. 16 Ladder line dimensions

$$\Theta_r = \Theta + r \ 2\pi/N \ ; \qquad r = 0, 1, \ldots..N-1$$

and the total voltage and current on the mth conductor is

$$\begin{aligned} (V_m)_r &= (A_1 \cos ky + A_2 \sin ky)_r \exp\left[j(wt-m\Theta_r)\right] \\ (I_m)_r &= j\,Y(\Theta)(-A_1 \sin ky + A_2 \cos ky)_r \exp\left[j(wt-m\Theta_r)\right] \end{aligned} \tag{37}$$

where $k = \frac{2\pi}{\lambda} = \frac{w}{c}$ and y is the coordinate measured along the conductors.

(a) Consider an ideal comb structure with fingers of length $h = \frac{\lambda}{4}$, and period L. Then r = 1 and

$$\begin{aligned} V_m &= (A_1 \cos ky + A_2 \sin ky) \exp\left[j(wt-m\theta)\right] \\ I_m &= j\,Y(\theta)(-A_1 \sin ky + A_2 \cos ky) \exp\left[j(wt-m\theta)\right] \end{aligned} \tag{38}$$

The current and voltage boundary conditions are

$$V_n\left(-\frac{h}{2}\right) = 0 \qquad \text{and} \qquad I_n\left(\frac{h}{2}\right) = 0.$$

Inserting these conditions into the relations for V_m and I_m and eliminating the constants gives the dispersion characteristic for the comb structure:

$$\tan^2 \frac{kh}{2} = 1 \tag{39}$$

This is a straight line, indicating no propagation. The voltage distribution is given by

$$V_m = A(\tan \frac{kh}{2} \cos ky + \sin ky) \exp\left[j(wt-m\theta)\right] \tag{40}$$

The mean stored energy per unit length of each conductor is given by

$$W_s = \frac{1}{c}\overline{|V_m|^2}\, Y(\theta)$$
$$= \frac{A^2}{2c}\sec^2\left(\frac{kh}{2}\right) Y(\theta) \qquad (41)$$

(b) Consider now the loaded comb structure shown in fig. 16. The structure is divided into two regions. The conductors have characteristic admittance $Y_1(\theta)$ in region (1) and $Y_2(\theta)$ in region (2). The current and voltages in the two regions are

$$(V_m)_1 = (A_1 \cos ky + A_2 \sin ky) \exp\left[j(wt-m\theta)\right]$$
$$(V_m)_2 = (A_3 \cos ky + A_4 \sin ky) \exp\left[j(wt-m\theta)\right] \qquad (42)$$

$$(I_m)_1 = j\, Y_1(\theta)(-A_1 \sin ky + A_2 \cos ky) \exp\left[j(wt-m\theta)\right]$$
$$(I_m)_2 = j\, Y_2(\theta)(-A_3 \sin ky + A_4 \cos ky) \exp\left[j(wt-m\theta)\right] \qquad (43)$$

Equating the voltages at the common boundary i.e. $y = 0$ gives $A_1 = A_3$. Equating the currents at the common boundary gives

$$A_4 = A_2 \frac{Y_1(\theta)}{Y_2(\theta)} \qquad (44)$$

Substituting for A_3 and A_4 in (42) and (43) and applying the boundary condition for region 1, $(I_m)_1 = 0$ at $y = h_1$ gives

$$\frac{A_1}{A_2} = \frac{Y_1(\theta)}{Y_2(\theta)} \cot kh_1 \qquad (45)$$

Similarly using the boundary condition for region 2, i.e. $(V_m)_2 = 0$ at $y = -h_2$

$$\frac{A_1}{A_2} = \frac{Y_2(\theta)}{Y_1(\theta)} \tan kh_1 \qquad (46)$$

The dispersion characteristic is therefore

$$\left\{\frac{Y_1(\theta)}{Y_2(\theta)}\right\}^2 = \tan kh_1 \tan kh_2 \qquad (47)$$

The group velocity may then be determined by using the formula $v_g = L\frac{dw}{d\theta}$. The energy flow P follows from the formula $P = v_g W$ where W

is given by equation (41) and

$$W = \frac{l}{L} \cdot W_s \cdot h \,. \tag{48}$$

(c) Meander line. The meander line is shown in fig. 16(c). It is a copper tape wound back and forth forming the centre conductor of a co-axial system. It thus resembles a helix. The meander line has a period of 2L, i.e. the boundary conditions are repeated for every second conductor. For thin tapes and large gaps the successive tapes are not coupled to each other and to an approximation, propagation may be described by a TEM wave moving along the tape. The group velocity can then be obtained from geometry and is

$$g = \frac{C}{1 + h/(a + b)}$$

indicating a linear dispersion characteristic. However this is a crude approximation. In practice the successive conductors are coupled. This becomes important when the effective length of a tape in a period is of the order of a half wavelength. A periodic structure type characteristic is then superimposed on the geometrical linear dispersion curve for this part of the frequency range. A much lower group velocity should result in this region.

The dispersion curve and other characteristics of the meander line can be obtained by using the method outlined for any array of parallel conductors. Since the boundary conditions are repeated for every second conductor, two TEM waves are required to describe the propagation. The boundary conditions are

$$V_{2n}(0) = V_{2n+1}(0)$$
$$I_{2n}(0) = -I_{2n+1}(0)$$
$$V_{2n}(h) = V_{2n-1}(h)$$
$$I_{2n}(h) = -I_{2n-1}(h)$$

Part V - Fabrication of Comb Structures and Meander Lines

Uniformity is an important characteristic of a slow wave structure. Any irregularities in the periodicity of the structure lead to reflections and hence to attenuation. The pass band is marred by peaks due to internal resonance. It is thus necessary not only to obtain high Qs but also to fabricate the structure to close tolerances.

Printed circuit techniques were used for construction. A black and white drawing, ten times as large as the required structure was made (a scale factor of 10:1). This serves to relax the drawing tolerances. A negative of the drawing was then produced. Standard photo-etching techniques were used to reproduce the circuit from the negative on to a copper clad laminate. Kodak photo resist, developer and dye were used. The etchant was a concentrated solution of ferric chloride. It was estimated that a dimensional tolerance of .001 inch could be obtained.

It is essential that the dielectric base material for the laminates has low losses at microwave frequencies. The best base material available for this purpose is teflon (polytetrafluoethylene). This can be obtained in both rigid and flexible forms. It has a dielectric constant between 2.64 - 2.89, a dissipation factor of 0.004 at 8500 Mc/s, and is reputed not to crack or deteriorate at extremely low temperatures. However, teflon is quite expensive. Other low loss base materials are bakelite, rexolite and epoxy resinglass. The last was selected because of its availability. It has a dielectric constant of approximately 5 and a dissipation factor slightly greater than that of teflon. The laminate used had a base thickness of 0.06 inches and the thickness of copper was .004 inches.

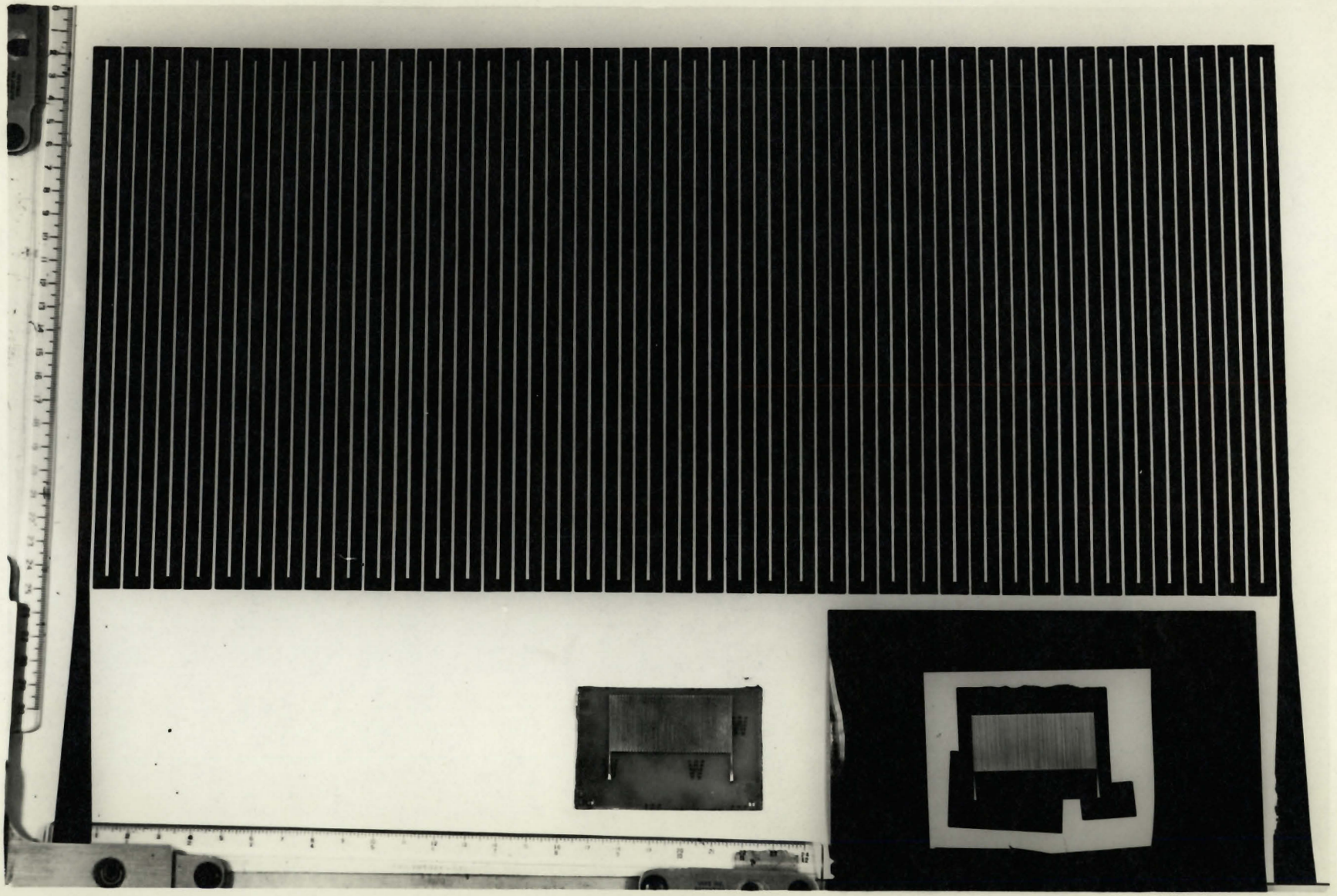

Fig. 9 Drawing, negative and the completed structure

SECTION V

MEASUREMENTS AND RESULTS ON COMB STRUCTURES AND MEANDER LINES

Various measurements can be made on slow-wave structures. For application in travelling wave masers it is essential to know the pass band, the group velocity and its variation in the pass band; and the field configurations, especially the circular polarization of the magnetic field, around the structure. Measurements of other characteristics, such as input impedance, input VSWR and Q factor of the structure are secondary, but help in obtaining a complete description of the structure. In this research program, propagation along comb structures (fingers shorted by a rod Fig. 10d) and meander lines in the L band has been studied.

The first comb structures were made out of brass rods in the laboratory. Although these structures showed a sort of a pass band, large fluctuations in the output were obtained. Anamolous effects were also observed preventing any accurate measurements. Printed circuit techniques were then used. Except for one or two minor fluctuations, gradual decrease and increase of the output, in line with the variation of group velocity and attenuation, was obtained in the pass band. This indicates the importance of close tolerances in the periodicity of the structures.

Various types of coupling schemes were tried to match a 50 Ω co-axial cable to the structures. For the comb structure the probe coupling was found to be the best. The centre conductor of the 50 Ω cable was extended to form the first and the last fingers in the structure. Special 50 Ω probes were also made, so that the centre conductor was of the same size as the fingers. A broad band match could be obtained by making slight modifications of this probe. The best result was obtained when the length of the probe was slightly longer than the fingers of the structure. Loop coupling was

also tried, but was found to be inefficient. In another coupling scheme the centre conductor of the 50 Ω cable was extended and attached to the first comb. Coupling was satisfactory but the bandwidth was smaller than with a probe. On the whole, an input VSWR of 1.5 could be obtained for the comb structure. Energy was coupled from a cable into a meander line by tapering the ends of the line to the size of the centre conductor of the co-axial cable. For a good match this taper should be gradual. An input VSWR of 1.7 was obtained in this case.

The insertion loss of the structures at different frequencies was also measured. This gave an indication of the pass and attenuation bands of the structure. A typical observation, for a comb structure, is shown in fig. 18. A comb structure of length 5 cm showed a loss of 2-5 db in the pass band while a meander line of the same length had a 5 db loss. In actual maser operation, at liquid helium temperatures, the losses will be substantially decreased. Small fluctuations observed due to internal resonances will also be suppressed by the nonreciprocity of the system.

An interesting behaviour was observed in the comb structure. The high frequency cutoff was quite sharp whereas the low frequency cutoff was gradual. This can be observed from the insertion characteristic: and may be explained by looking at the cutoff configurations in fig. 17 which shows a comb structure with two ground planes. It will be observed that the ground planes do not affect the high frequency cutoff (π mode). As the frequency is decreased, the phase shift between fingers decreases and the field lines tend to 'open up'. However, if the ground plane is present, a sharp low frequency cutoff (zero phase shift between fingers) occurs when the electric field lines suddenly switch over to the plane. Thus if the plane is too near the fingers the characteristics of the structure are altered. If no ground planes are present the cutoff will be gradual.

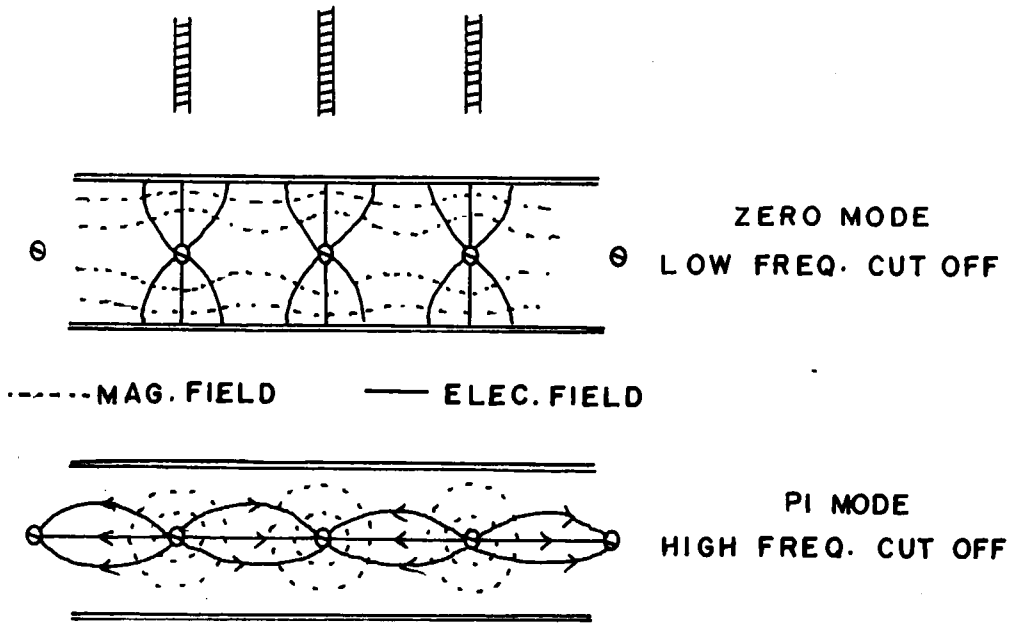

Fig. 17 Cutoff frequency TEM mode patterns

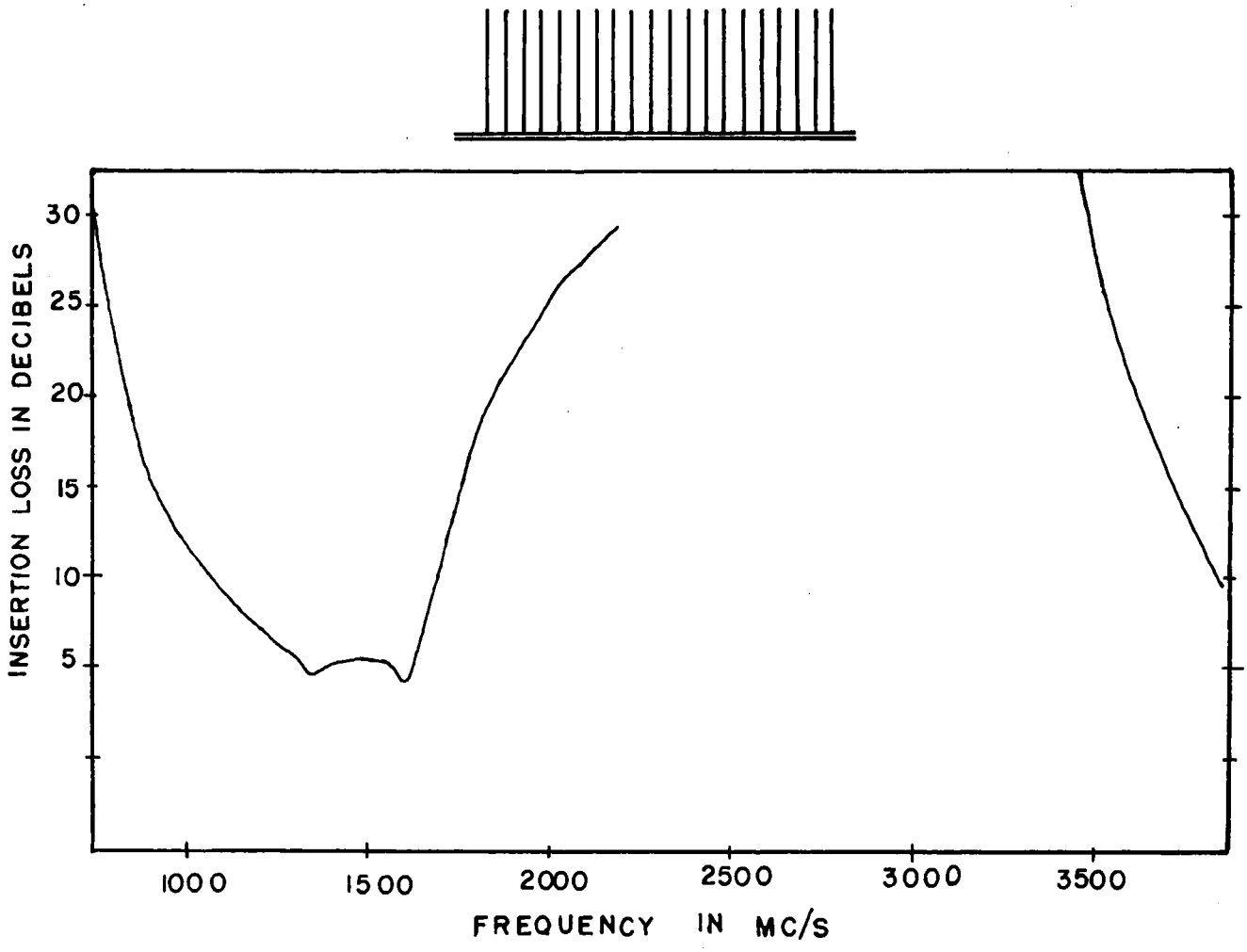

Fig. 18 Insertion loss characteristic of comb structure

1. Measurement of Group Velocity

Two types of method exist for the measurement of group velocity - indirect and direct. The indirect method consists in determining the dispersion characteristic of the structure. As mentioned before, the group velocity is then the slope of this curve. Although the method is indirect, it gives a good insight into the operation of the structure. The direct measurement is a phase measurement and consists in measuring either the time delay through the structure of the variation in phase shift through the structure with frequency.

(a) Experimental determination of the dispersion characteristic. The simplest method consists in shorting the structure at one end and measuring the wavelength along the structure, for different frequencies in the pass band. Since

$$v_g = \frac{dw}{d\beta} = 2\pi \frac{df}{d(\frac{2\pi}{\lambda_g})} = \frac{df}{d(1/\lambda_g)}$$

a plot of frequency against $\frac{1}{\lambda_g}$ gives the dispersion characteristic. However the probe or loop, sampling the field, detects the total field of all the space harmonics, whereas generally a determination of the wavelength of the space harmonic with the largest amplitude is all that is required. Although the fundamental is generally most intense, the harmonics may be large enough to mask its distribution. Thus this method is limited to structures which have a space harmonic with an amplitude much larger than that of the others. Any irregularities in the structure tend to radiate, further distorting the fields. This measurement was carried out on a comb structure by placing a copper plate normal to the structure and midway between two fingers of the comb. Although variations in the standing wave pattern were observed, no consistency in the distance between two modes was obtained. The method was therefore dropped.

Another method, particularly suited for enclosed structures, consists in short circuiting the structure at both ends and searching for the resonant frequencies. If the structure has n sections, the multiple cavity formed will have (n + 1) resonances whenever the total phase shift is $m\pi (m = 0, 1, 2, \ldots\ldots n)$. These resonances form a group of (n + 1) frequencies in the restricted pass band, the modes being clustered in the vicinity of the 0 and π modes (low and high frequency cutoff) and more widely spaced in between. The dispersion characteristic can be constructed if the phase shift corresponding to each resonance is known. The problem is trivial if all the resonances are detected. However, this is not always possible, especially near the cutoff regions where attenuation is high. The phase shift corresponding to each resonance may be determined if possible by probing the field pattern. Another method due to Nalos [17] consists in moving a small perturbing object along the structure in a region of maximum electric field and minimum magnetic field, and noting the shift in resonance frequency. A voltage node is indicated when there is no shift in the resonance frequency. These methods fail if the field is not well defined. Other techniques consist in varying the number of sections and the method of short circuiting the structure. If large numbers of sections are taken, the adjacent resonances get mixed up and are less distinct, especially near the cutoff. If a few resonances in succession are available it is still possible to determine the group velocity for that region of the pass band.

The method was tried with comb structures by placing two polished copper plates at the ends of the structure. The cavity was excited by a signal generator and a poor coupling to prevent distortion of the 'cavity' fields. The plates were placed at the planes of symmetry of the system so as not to excite any other modes. Very few resonances were obtained, especially near the low cutoff frequency. Even some of the observed resonances were exceedingly weak. It was also found difficult to couple into the structure without

disturbing the fields.

(b) Measurement of group velocity by measuring the time delay through the slow wave structure.

This is a method particularly suited for structures used in travelling wave masers, as the group velocity may be determined under operating conditions. Use is made of the fact that the group velocity is the velocity of motion of the modulation envelope (- the group). A schematic diagram of the circuit is shown in fig. 19. The circuit is a set up essentially for measuring the phase shift θ through the structure. The time delay is then given by θ/w where w is the angular modulating frequency. Since the time delay, through the structure, is independent of the modulating frequency, varying w will vary the phase shift θ . The measurement consists in adjusting the modulating frequency to a value $w = w_1$ so that a straight line is obtained. This corresponds to a phase delay of $n\pi$, where n is a positive integer, and a time delay of $\frac{n\pi}{w_1}$. The observation is repeated without the structure. In this case, the straight line obtained for an angular frequency $w = w_o$ corresponds to a phase shift $m\pi$ where m is another positive integer. The time delay is then given by

$$t = \frac{n\pi}{w_1} - \frac{m\pi}{w_o}$$

If l is the length of the structure the group velocity is given by

$$v_g = \frac{l}{t} = \frac{l}{\frac{n\pi}{w_1} - \frac{m\pi}{w_o}} = \frac{2l}{\frac{n}{f_1} - \frac{m}{f_o}}$$

Integers m and n may be individually determined by observing the difference in modulating frequency Δw, for the (say) m and (m + 1)th straight line. Then

$$m = \frac{w_o}{\Delta w}$$

The accuracy of the measurement increases, the higher the modulating frequency.

The experimental set up used a Hewlett Packard 614A, Ultra High frequency signal generator for the signal frequency. Isolation from the rest of the circuit was obtained with a 10 db attenuator and a ferrite isolator. A General Radio crystal modulator was used to provide sinusoidal modulation. The modulated signal was detected, after propagation through the structure, by a silicon diode detector. The detected radio frequency signal was amplified by a Tektronix wide band (bandwidth 0-12 Mc/s) preamplifier, and applied to the vertical section of a tektronix type 536 oscilloscope. The horizontal section was fed directly from the radio frequency signal generator. Two identical CA plug-in units were used in the horizontal and vertical sections of the oscilloscope. The CA plug-in units have a 15 Mc/s band width and the internal amplifiers of the scope a 10 Mc/s bandwidth.

Without the structure the relative time delay in the modulation circuit was found to be 0.2 μs, the first straight line being obtained around 2.5 Mc/s. Measurements were taken for n = m = 1 to keep to a minimum any unwanted relative phase shifts produced in the modulator, detector and preamplifier.

Measurements were carried out on the meander line, straight comb structure and a skewed comb structure. The results are shown in figs. 20, 21, and 22. The general shape of thecurves is what one would expect from qualitative reasoning. For the meander line, the group velocity is high at the low frequency end corresponding to the geometric slowing. The steep rise at the low frequency end in fig. 20 is the transition from the linear geometrical characteristic to the nonlinear dispersion characteristic. However, at higher frequencies the length of the individual conductors (h) corresponds to $\frac{\lambda}{4}$ and a much lower group velocity results. In this region a slowing factor ($s = c/v_g$) ranging from 100 to 300 was obtained. As was expected, the

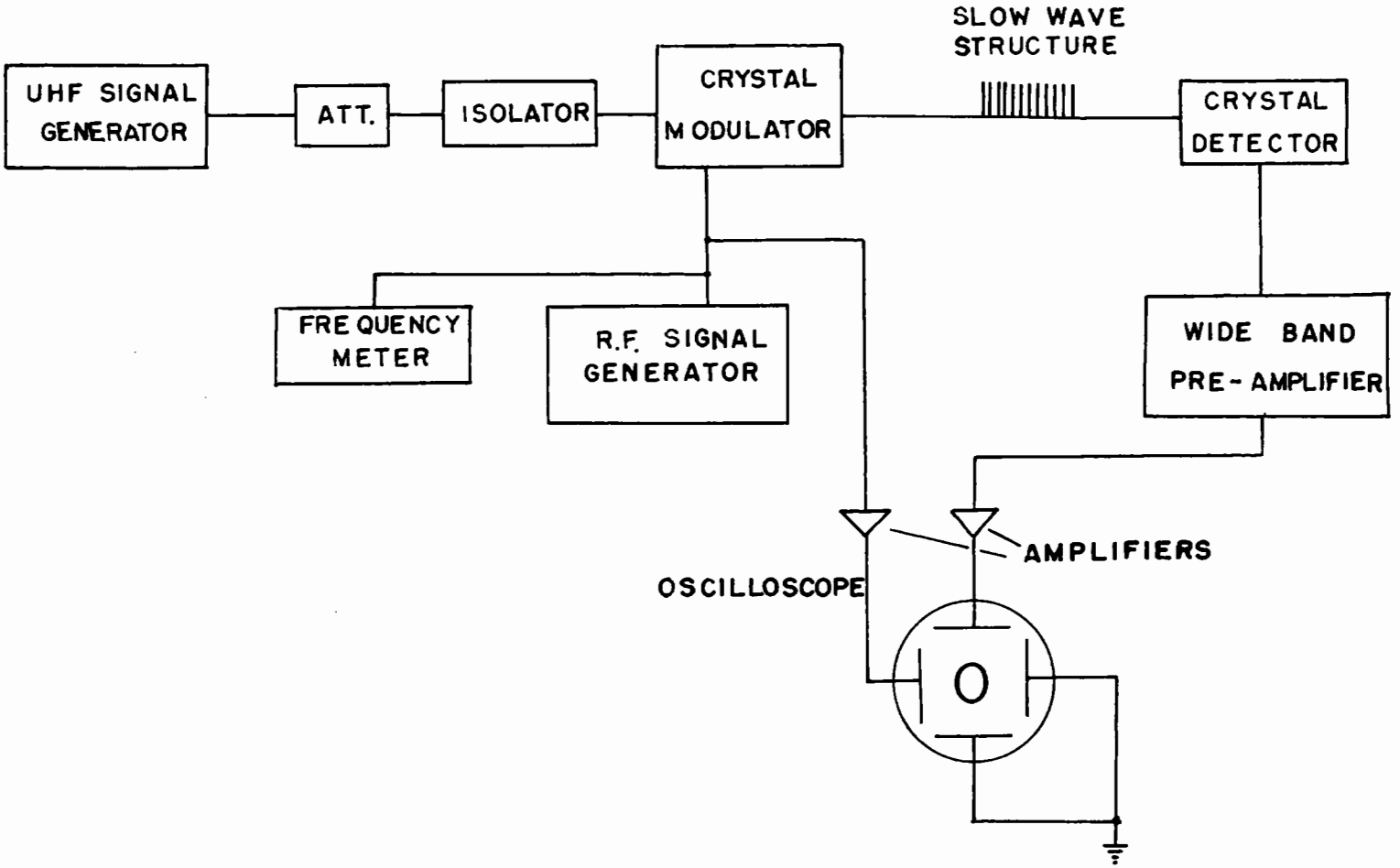

Fig. 19 Block diagram for the measurement of group velocity

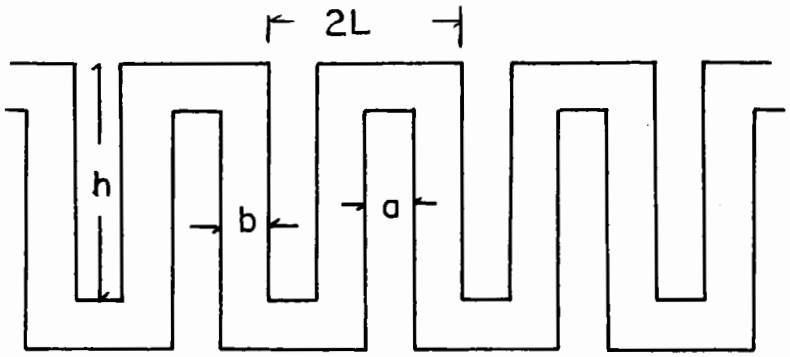

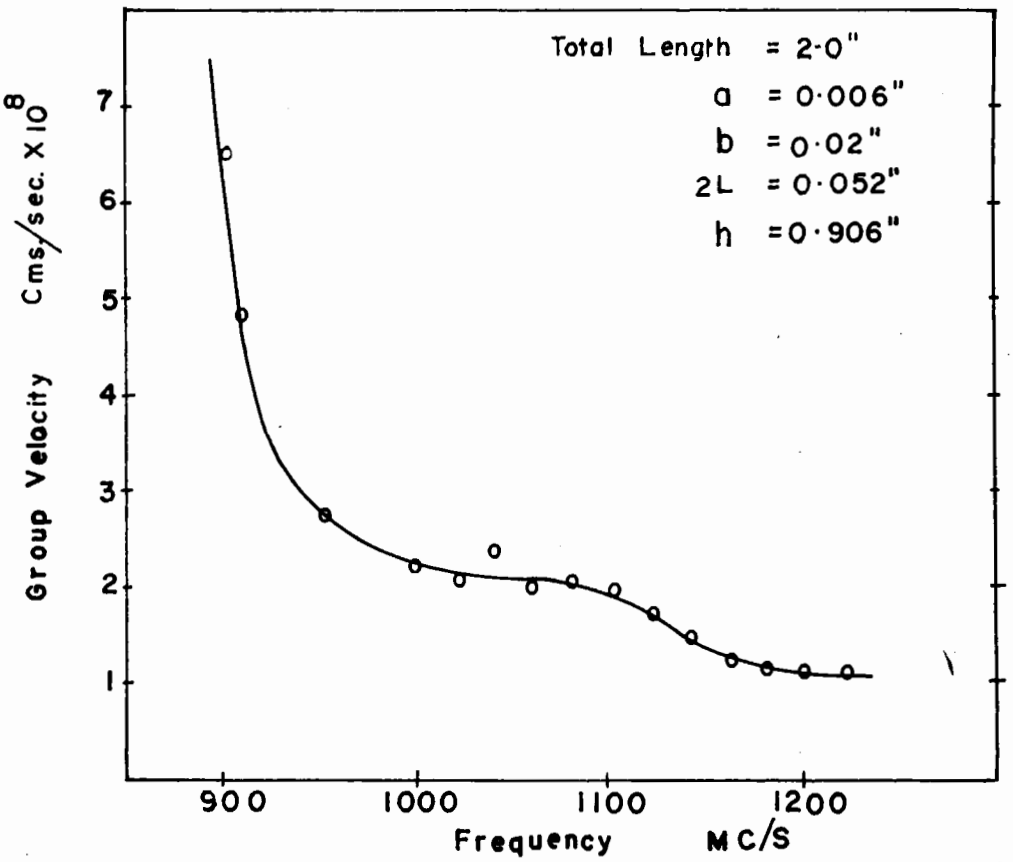

Fig. 20 Variation of Group Velocity with frequency for a meander line

Total Length = 0·75"

L = 0·063"

h = 1·2"

a = 0·032"

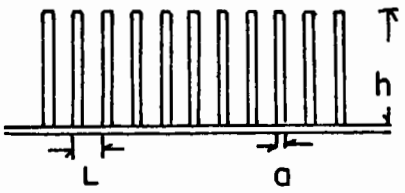

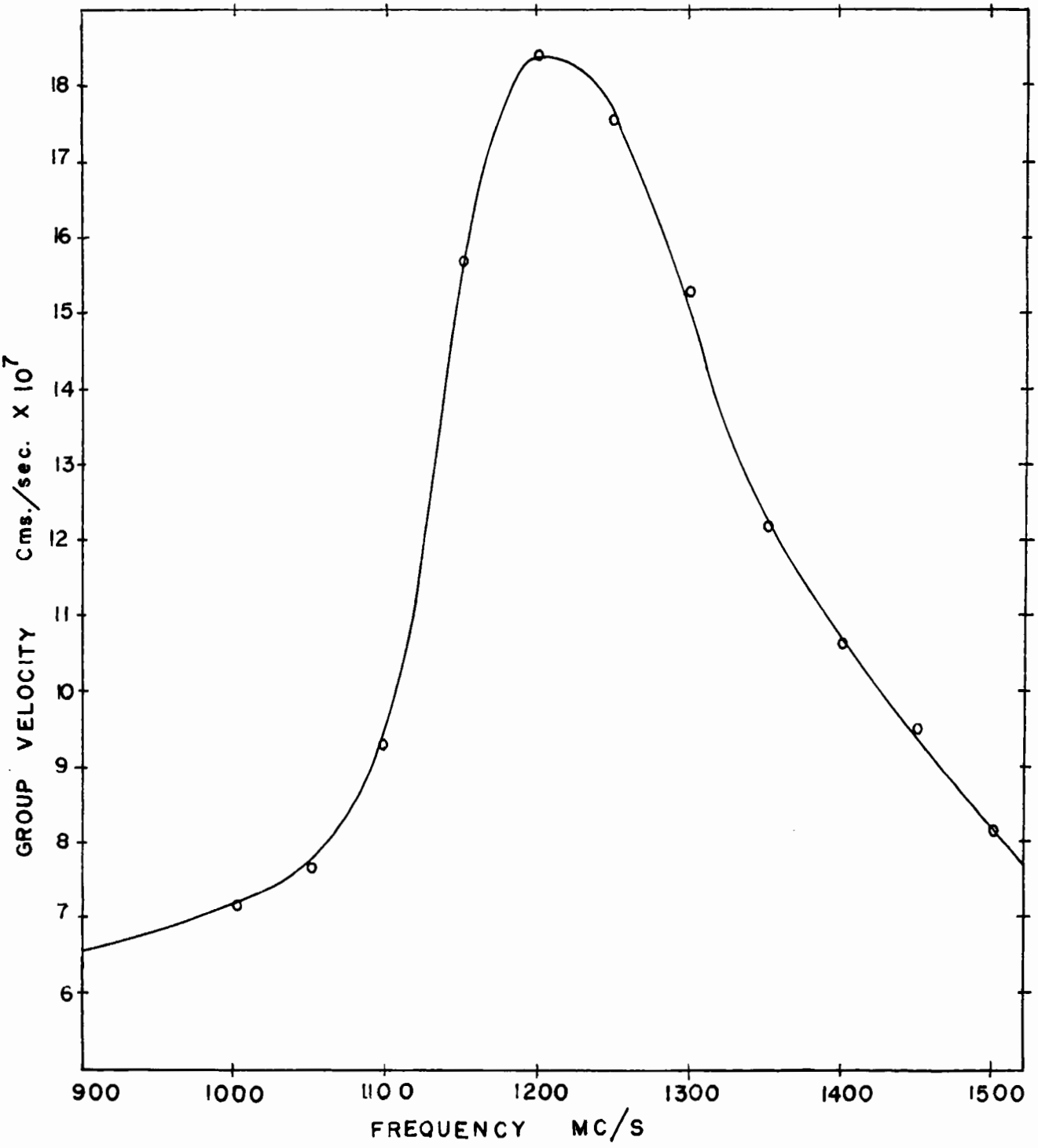

Fig. 21 Variation of Group Velocity in the Pass Band of a comb structure

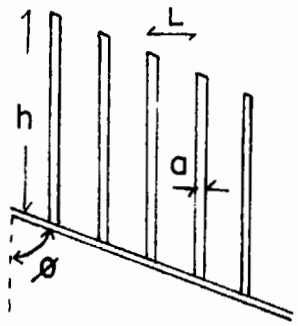

Total Length = 0·75"
L = 0·063"
a = 0·032"
ø = 60°
h = 1·1"

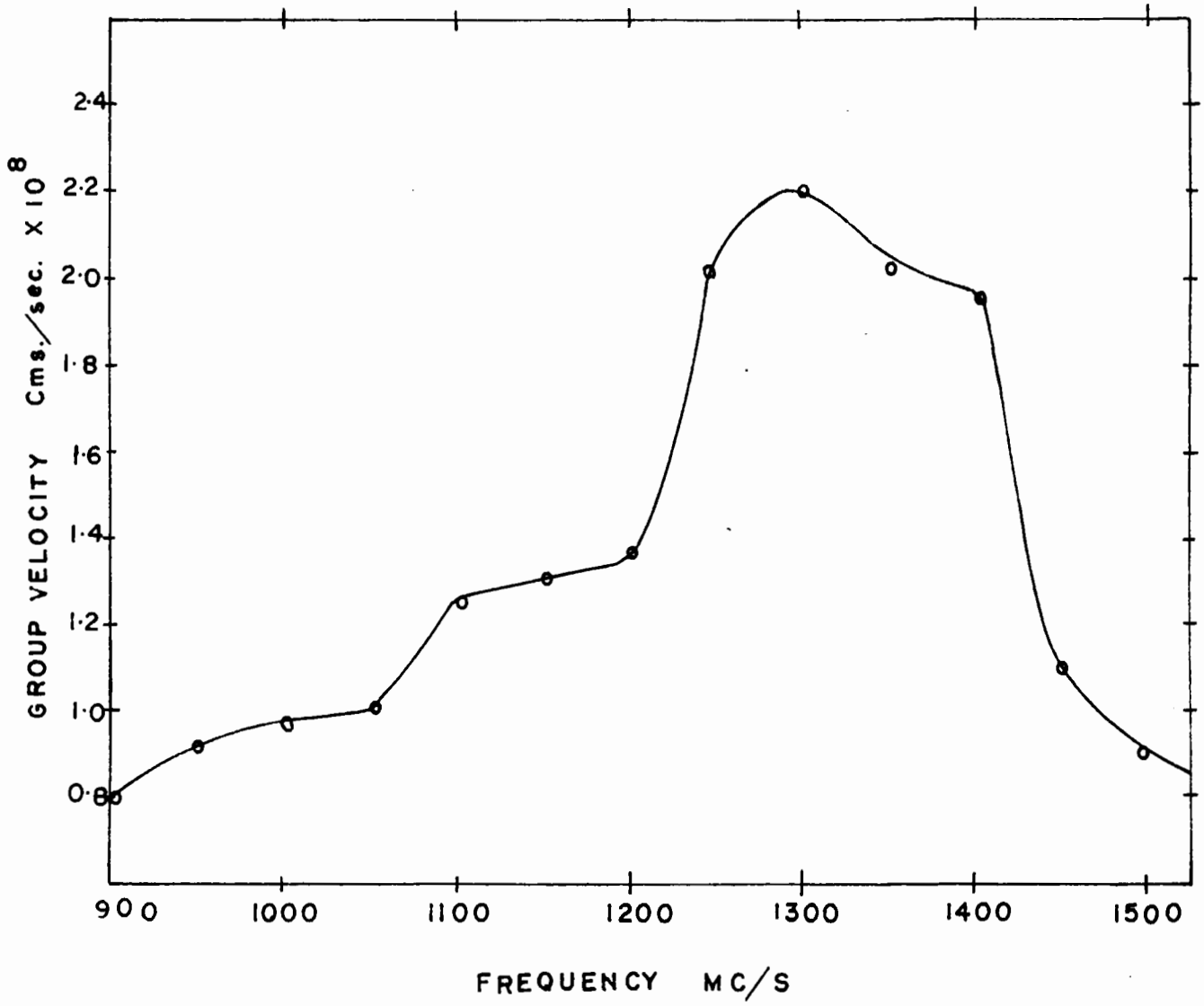

Fig. 22 Variation of Group Velocity in the Pass band of a skewed comb structure

comb structure produced high slowing. However, the slowing factor was found to vary over a wide range and little constancy was observed. A somewhat improved variation was obtained for a skewed structure where a reasonably constant slowing was obtained over a 200 Mc/s band. The slowing obtained was slightly less compared to a straight comb structure. This can be explained, since the skewing further reduces the magnetic coupling without much affecting the electric coupling. A meander line can be skewed in a similar manner to adapt it for use with a solenoid.

2. Measurement of the circular polarization of the magnetic field

This measurement has not been carried out but a brief outline of the method to be used is given. As mentioned earlier, comb structures have regions of contra rotating circular polarized magnetic field, above and below the plane of the combs. This can be observed from fig. 13, by noting the variation of the magnetic field vectors at points A and A^1 as the wave travels along the comb. The circular polarization of the magnetic field is measured by probing the magnetic field by means of a ferrite sphere at resonance. A dc magnetic field has to be applied normal to the plane of polarization, i.e. along the fingers.

The measurement consists in placing a well matched structure in the required dc magnetic field (strength depending on ferrite sample used). It is essential that the structure be well matched since poor matches result in standing wave admixtures which do not possess circular components. The ferrite sphere may be placed in a capillary glass tube, which may then be moved across the structure by an improvised depth gauge micrometer drive. The strength of ferrimagnetic absorption is proportional to the circularly polarized magnetic r.f. field, where the circular polarization refers to a plane perpendicular to the applied dc field. Decrease in the output power from the structure would give the absorption.

The ferrite sample used at the Bell Telephone Laboratories was a 20 mil sphere of polycrystalline gallium substituted yttrium iron garnet, which had a saturation magnetization of 400 gauss, and a resonance line width of approximately 20 oersted. An advantage of using a low magnetization material is that it keeps the perturbation of the field small. An advantage of low line width is that one is able to display the resonance signal directly on a scope using 60 cycle field modulation superimposed on the d.c. field. A meter can also be used, although it may not be possible to distinguish the wanted signal from the hum.

CONCLUSIONS

In this dissertation, propagation along structures consisting of arrays of parallel conductors was studied. Propagation along modified comb structures and meander lines was experimentally examined. Various other possibilities for travelling wave masers were also considered.

The solenoid was considered as a possible replacement for the magnet. Besides being slightly cheaper and lighter in weight, the solenoid can be designed to accommodate longer structures. The disadvantages, as compared to magnets, are smaller and slightly less uniform magnetic fields, which are not serious drawbacks in travelling wave masers.

Comb structures are capable of producing high slowing. However, experiments still need to be performed to determine the effect of various parameters on slowing, so as to obtain a structure with constant slowing over a wide range of frequency. Skewed comb structures showed satisfactory results but the circular polarized component of the magnetic field round such a structure was not measured. It is hoped that 'wrapping' a skewed structure for use with a solenoidal dc magnetic field, will not greatly affect the characteristics.

Although meander lines produced reasonable amounts of slowing, it was found that the wave stuck quite closely to the structure and thus in actual maser operations would excite few spins in the crystal. They are therefore likely to produce smaller gains, as compared to comb structures.

Fletcher's analysis of interdigital circuits was extended to comb structures and meander lines. Only a outline of the theoretical method has been given and the theoretical dispersion curves are still to be compared with experimental results.

REFERENCES

(1) Mount and Begg: "Parametric Devices and Masers; an Annotated Bibliography." IRE Trans. M.T. and T. - 8, 222, March 1960.

(2) DeGrasse: "Slow wave structures for unilateral solid state maser amplifiers", 1958 IRE WESCON Conv. Rec. Pt. 3, 29, 1959.

DeGrasse, Schulz Du-Bois and Scovil: "Three level solid state travelling wave maser". B.S.T.J. 38, 305, 1959.

(3) Chang, Cromack and Siegman: "Cavity and travelling wave masers using ruby at S band" 1959 IRE WESCON Conv. Rec. Pt. 1, 142, 1959.

(4) Tenney, Roberts and Vartanian: "An S band travelling wave maser". 1959 IRE WESCON Conv. Rec. Pt. 1, 151, 1959.

(5) Siegman: "Travelling wave techniques in microwave measurements" 'Quantum Electronics' (Columbia Univ.)m p.597, 1960.

(6) Okwit, Arams and Smith: "Electronically tunable travelling wave maser at L and S bands". P. IRE (L), 2025, 1960.

(7) Butcher: "Travelling wave maser" RRE Journal 43, 1, 1959 April.

(8) Harvey: "Periodic and Guiding structures at microwave frequencies", IRE trans. M.T. and T. - 8, 31 Jan. 1960.

(9) Brillouin "Wave Propagation and Group Velocity" (Academic Press) 1960.

(10) Singer: "Masers" (J. Wiley), 1959, p.115.

(11) Szabo: "Investigations of magnetically focused electron beams", M.Sc. thesis. McGill, 1955.

(12) Fletcher: "Broadband interdigital circuit". P. IRE, 40, p.951, August 1952.

(13) Walling: "Interdigital and other slow wave structures", J. of El. and and Control III, 3, p.239, Sept. 1957.

(14) Mourier and Leblond: "Investigations of lines with periodic bar structure" parts I and II. Ann. Radio electricite (F), 9, p.180, 311, April 1954.

(15) Gardner, Jungerman, Lictenstein and Patten: "Production of a uniform magnetic field by a end corrected solenoid". Rev. of Sci. Inst. 31, 929, Sept 1960.

(16) Antler: "Superconducting Electromagnets", Rev. Scient. Inst. 31, 369, April 1960.

(17) Nalos: "Measurement of circuit impedance of periodically loaded structures by frequency perturbation", P. IRE 42, 1508, Oct. 1954.

APPENDIX I Calculation of the gain and power output of a travelling wave maser

From electro-magnetic theory we have

$$B = \mu_o(H + M_m) \tag{I-1}$$

where μ_o is the permeability of free space and M_m the magnetic moment per unit volume. The magnetic moment may be computed from the quantum mechanical treatment of the paramagnetic spin system. Equation (I-1) may also be written

$$\begin{aligned} \mu_o\mu_r H &= \mu_o(H + M_m) \\ M_m &= (\mu_r - 1)H \end{aligned} \tag{I-2}$$

where μ_r is relative permeability. Since magnetization of a specimen will not instantaneously follow a high frequency variation of the applied magnetic field, the susceptibility is defined as

$$\chi = \chi' - j\chi'' = \frac{M_m}{H} \tag{I-3}$$

The real part of the susceptibility χ', in phase with the field will produce reactive effects in the microwave circuit, while the imaginary part can produce loss or gain. From equations (I-2) and (I-3)

$$\mu_r = 1 + \chi' - j\chi'' \tag{I-4}$$

For a system with a small magnetic loss but no dielectric instruction, χ' is small compared to 1 ($\lesssim 10^{-3}$) and $\epsilon = 1$

$$\mu_r = 1 - j\chi'' \tag{I-5}$$

If an oscillating field H sin wt is applied, an in phase magnetization $\chi' H \sin wt$ and an out of phase magnetization $-\chi'' H \sin wt$ will result. The

energy absorbed or emitted is given by $\mu_o H \cdot \frac{dM_m}{dt}$ and hence the power absorbed or emitted by the material

$$P = \mu_o \frac{w}{2\pi} \int_o^{\frac{2\pi}{w}} H \frac{dM_m}{dt} dt$$

$$= \frac{w}{2\pi} H^2 \mu_o \int_o^{\frac{2\pi}{w}} w (\sin wt \chi' \cos wt + \chi'' \sin^2 wt) dt$$

$$\text{or} \qquad P = \frac{1}{2} w \mu_o \chi'' H^2 \qquad \text{(I-6)}$$

For a case where H varies sinusoidally with time and is given by a complex exponential

$$P = \frac{1}{2} w \mu_o \int H \cdot \chi'' \cdot H^* \, dA \qquad \text{(I-7)}$$

To calculate the gain, χ'' has to be determined. In general χ'' depends on the orientation of H and is a tensor. Rather than use the exact tensor representation, it is convenient to obtain a value for χ'' which reflects the magnetic field orientation. In a travelling wave maser circular polarized magnetic fields are used to excite the signal transition, and hence the susceptibility χ'' for circular polarization should be determined.

Consider the ionic states in a paramagnetic crystal. When transitions are excited by radiation of frequency f_{ij}, the rate of transitions between the i and j states is described by the transition probability w_{ij}. The transition probability due to the applied radiation is the same for upward and downward transitions, $w_{ij} = w_{ji}$. The energy absorbed from (or given to) the exciting field is one quantum, hf_{ij}, per transition. The power absorbed per unit volume is

$$P_{ij} = hf_{ij} w_{ij} (\rho_j - \rho_i) \qquad \text{(I-8)}$$

Here i denotes the higher energy state and ρ the density of ions in each particular state. Power is emitted rather than absorbed if the densities are "inverted", i.e. $\rho_i > \rho_j$. The transition probability, obtained from quantum mechanics is

$$w_{ij} = \frac{1}{4}\left(\frac{2\pi}{h}\right)^2 g(f) \left| \vec{H}^* \cdot \vec{M}_{ij} \right|^2 \qquad \text{(I-9)}$$

Here g(f) is a normalized function describing the line shape as a function of frequency, $\int g(f)df = 1$; the line is centred at f_{ij}. $\vec{H}$ is the exciting rf field and $\vec{M}_{ij}$ is the magnetic dipole moment associated with the transition from state i to j. The asterisk denotes the complex conjugate, i.e. a quantity having an opposite time dependance. Using Dirac's bracket notation, the dipole moment is defined quantum-mechanically by

$$M_{ij} = g\beta \langle j \,|\, \vec{S} \,|\, i \rangle \qquad \text{(I-10)}$$

Here g ($\simeq 2$) is the spectroscopic splitting factor, β ($= \frac{\mu eh}{4m\pi}$) is the Bohr magneton, $\vec{S}$ the vector spin operator whose components are S_x, S_y and S_z. Both $\vec{H}$ and $\vec{M}_{ij}$ are varying in time like exp ($iw_{ij}t$) and there may be phase differences between the components of $\vec{M}_{ij}$ and $\vec{H}$. If the dc magnetic field is in the z direction, the magnetic moment vector rotates in the x-y plane. M_{ij} then has components M_x and M_y, equal in amplitude but 90° out of phase. Maximum transition probability occurs if M_{ij} and H have the same polarization. Thus in this case a transition is excited by a circularly polarized rf magnetic field of the same sense. Then for a circularly polarized magnetic field $H_x = (\frac{1}{\sqrt{2}})$ H cos wt, $H_y = \pm(\frac{1}{\sqrt{2}})$ H Sin wt and $S = (\frac{1}{\sqrt{2}})S_{\pm}$ where positive and negative circular polarization are assumed indicated by S+ and S-. Assuming positive circular polarization causes the transition, (I-9) becomes

$$w_{ij}(S_+) = \frac{1}{2}\left(\frac{\pi g\beta}{h}\right)^2 g(f) \left| \langle j \,|\, S_+ \,|\, i \rangle \right|^2 H_+^2 \qquad \text{(I-11)}$$

Comparing (I-8) and (I-6)

$$\chi_+'' = \frac{\pi}{2\mu_o h} (g\beta)^2 (\rho_j - \rho_i) g(f) \left| \langle j \; S_+ \; i \rangle \right|^2 \qquad \text{(I-12)}$$

χ_+'' can thus be calculated if the spin Hamiltonian and hence the wave functions of the crystal are known. The power output and gain of the travelling wave maser are given by equations (I-6) and (12).

APPENDIX II Noise Figure and Noise Temperature

Following I.R.E. standards the noise figure F (or noise factor) of an amplifier may be defined as the noise power appearing at the output divided by that portion of the noise power due to the input generator which is maintained at a temperature T_o of 290°K (Standard Noise temperature).

Noise figure in decibels = $10 \log_{10} F$ (II-1)

One disadvantage of using the noise figure as defined above for low noise amplifiers, is that the input signal generator must be at 290°K. It is quite difficult to measure the very small contribution of maser noise to the output when the input generator operates at a much higher level. Consequently it is often convenient to use the concept of noise temperature.

Consider an actual amplifier. Then

$$F = \frac{(N_p)_{out}}{(N_p)_{ideal}} = \frac{(N_p)_{out}}{kT_o \int_o^\infty G(f)df} \qquad \text{(II-2)}$$

where $(N_p)_{out}$ is the output noise power and G(f) the power gain of the amplifier at a frequency, f. The available output noise power may be written as

$$(N_p)_{out} = kT_o \int_o^\infty G(f)df + (N_p)_A \qquad \text{(II-3)}$$

where $(N_p)_A$ is the noise due to the amplifier, and may be due to many different types of noise sources within the amplifier in addition to thermal noise sources. Nevertheless one may define a temperature

$$T_N = \frac{(N_p)_A}{k \int_o^\infty G(f)df} \qquad \text{(II-4)}$$

so that $$(N_p)_{out} = k(T_o + T_N) \int_o^\infty G(f)df \qquad \text{(II-5)}$$

With the help of (II-2) and (II-5)

$$T_N = (F - 1)T_o \qquad \text{(II-5)}$$

T_N is defined as the effective noise temperature of the amplifier and is a direct measure of its noisiness. It does not correspond to the ambient temperature of the amplifier. If the generator temperature is T_1 we shall get a different noise figure F_1 but

$$T_N = (F_1 - 1)T_1 \qquad \text{(II-7)}$$

The advantage of the noise temperature as a figure of merit is clear from these equations: it is independent of the temperature of the source.

APPENDIX III Characteristic Admittance of a Single Conductor in an array. (12)

Suppose that the voltages on successive conductors in a plane (x, z) are related by (leaving out time variation)

$$V_m = V_{m-1} \exp(-j\theta) = A_o\, e^{-j\phi}\, e^{jm\theta} \qquad \text{(III-1)}$$

where $\phi = \frac{2\pi}{\lambda}$ and θ is the phase difference between fingers. The line is divided into three regions 1 , 2 and 3 (see fig. 16) assuming a ground plane in region 3, at a distance w. It is also assumed that the electric field between fingers in region 1 is uniform. The characteristic admittance Y (θ) is defined by

$$Y(\theta) = \frac{I_m}{V_m} \qquad \text{(III-2)}$$

$$E_{z1} = \frac{V(m+1) - V_m}{\ell} = \frac{A_o}{\ell}\, e^{-j\phi}\, e^{-jm\theta}\,(e^{-j\theta} - 1)$$

$$= \frac{A_o}{\ell}\, e^{-j\phi}\, e^{-j(m+\frac{1}{2})\theta}\,(e^{-j\theta/2} - e^{j\theta/2})$$

$$= -2j\,\frac{A_o}{\ell}\, e^{-j\phi} \sin\theta/2\; e^{-j(m+\frac{1}{2})\theta}$$

$$= E_o\, e^{-j\phi}\, e^{j(m+\frac{1}{2})\theta}$$

$$\text{for } E_o = -2j\,\frac{A_o}{\ell} \sin\frac{\theta}{2} \qquad \text{(III-3)}$$

$$\text{and} \qquad (m+\tfrac{1}{2})L - \frac{\ell}{2} < z < (m+\tfrac{1}{2})L + \frac{\ell}{2}$$

The electric fields in regions 2 and 3 must be a superposition of waves having the correct periodicity in the z direction and satisfying the boundary conditions at x = w and x = $-\infty$. The origin of x is assumed to be one edge of the finger for region 2 and the other edge for region 3 . The field in regions 2 and 3 will be that due to all the harmonics and will vary in the x-direction also.

Thus we may write

$$E_{z2} = \sum_{n=-\infty}^{\infty} F_{n2} \; e^{+|\theta + 2\pi m| \, x/L} \; e^{-j\phi} e^{-j(\theta + 2\pi m)z/L} \qquad \text{(III-4)}$$

where F_{n2} is the amplitude of the nth spatial harmonic in region 2. E_{z2} thus vanishes for $x = -\infty$. Also

$$E_{z3} = \sum_{n=-\infty}^{\infty} F_{n3} \; \frac{\sin h \left\{(\theta + 2\pi m)\frac{W-x}{L}\right\}}{\sin h \left\{(\theta + 2\pi m)\frac{W}{L}\right\}} \; e^{-j\phi} \, e^{-j(\theta + 2\pi m)z/L} \qquad \text{(III-5)}$$

which vanishes for $x = w$. For continuity we equate the electric fields at the boundaries of the regions 1, 2 and 3, i.e. $x = 0$.

$$\sum_n F_{n2} \, e^{-j(\theta + 2\pi m)z/L} = \sum_n F_{n3} \, e^{-j(\theta + 2\pi m)z/L}$$

$$= \begin{cases} E_o \, e^{-j(m+\frac{1}{2})\theta} & \text{for } (m + \tfrac{1}{2})L - \frac{\ell}{2} < z < (m + \tfrac{1}{2})L + \frac{\ell}{2} \\ 0 & \text{for } mL - \frac{L-\ell}{2} < z < mL + \frac{L-\ell}{2} \end{cases}$$

Multiplying both sides by $e^{+j(\theta + 2\pi m)z/L}$ we have a term of the L.H.S.

$$= \int_{mL}^{(m+1)L} e^{j(\theta + 2\pi m)z/L} \sum_n F_{n2} \; e^{-j(\theta + 2\pi m)z/L} \, dz$$

$$= \int_{mL}^{(m+1)L} e^{j2\pi m \, z/L} \sum_n F_{n2} \; e^{-j2\pi m \, z/L} \, dz$$

There is only one non zero term in the series

$$= LF_{n2}$$

$$F_n \equiv F_{n2} = F_{n3} = \frac{1}{L} E_o \, e^{-j(m+\frac{1}{2})\theta} \int_{(m+\frac{1}{2})L - \frac{\ell}{2}}^{(m+\frac{1}{2})L + \frac{\ell}{2}} e^{\, j(\theta + 2\pi m)z/L} \, dz$$

$$= (-1)^n \frac{\ell}{L} E_o \; \frac{\sin(\theta + 2\pi m)\frac{\ell}{2L}}{(\theta + 2\pi m)\ell/2L} \qquad \text{(III-5)}$$

The remaining field components are found with the aid of Maxwell's equation.

$$H_{x1} = \sqrt{\frac{\epsilon}{\mu}}\ E_o\ e^{-j\phi}\ e^{-j(m+\frac{1}{2})\theta} \qquad \text{(III-6)}$$

$$\text{for} \quad (m+\tfrac{1}{2})L - \frac{\ell}{2} < z < (m+\tfrac{1}{2})L + \frac{\ell}{2}$$

$$E_{x2} = j \sum F_n\ e^{\{\theta + 2\pi m|\, x/L\}}\ e^{-j\phi}\ e^{-j(\theta + 2\pi m)z/L} \qquad \text{(III-7)}$$

$$H_{x2} = \sqrt{\frac{\epsilon}{\mu}} \sum F_n\ e^{\{\theta + 2\pi m|\, x/L\}}\ e^{-j\phi}\ e^{-j(\theta + 2\pi m)x/L} \qquad \text{(III-8)}$$

$$H_{z2} = -j \sqrt{\frac{\epsilon}{\mu}} \sum F_n\ e^{\{\theta + 2\pi m|\, x/L\}}\ e^{-j\phi}\ e^{-j(\theta + 2\pi m)z/L} \qquad \text{(III-9)}$$

$$E_{x3} = -j \sum F_n \frac{\cos h\{(\theta + 2\pi m)\frac{w-x}{L}\}}{\sin h\{(\theta + 2\pi m)w/L\}}\ e^{-j\phi}\ e^{-j(\theta + 2\pi m)z/L} \qquad \text{(III-10)}$$

$$H_{x3} = \sqrt{\frac{\epsilon}{\mu}} \sum F_n \frac{\sin h\{(\theta + 2\pi m)\frac{w-x}{L}\}}{\sin h\{(\theta + 2\pi m)w/L\}}\ e^{-j\phi} e^{-j(\theta + 2\pi m)z/L} \qquad \text{(III-11)}$$

$$H_{z3} = j\sqrt{\frac{\epsilon}{\mu}} \sum F_n \frac{\cos h\{(\theta + 2\pi m)\frac{w-x}{L}\}}{\sin h\{(\theta + 2\pi m)w/L\}}\ e^{-j\phi}\ e^{-j(\theta + 2\pi m)z/L} \qquad \text{(III-12)}$$

By using equations (III-6, 9, 12, and 3) the current flowing in the fingers can be calculated by integrating the tangential magnetic field around the periphery of a finger.

$$I_m = d\left\{H_{x1}(m+\tfrac{1}{2}) - H_{x1}(m-\tfrac{1}{2})\right\} + \int_{mL-(L-\ell)/2}^{mL+(L-\ell)/2} (H_{z2} - H_{z3})_{x=0}\, dz \qquad \text{(III-13)}$$

Integrating equation (III-13) and remembering the definition of $Y(\theta)$, (III-2) we obtain

$$Y(\theta) = \sqrt{\frac{\epsilon}{\mu}}\left[4\frac{d}{\ell}\sin^2\frac{\theta}{2} + \frac{L-\ell}{L}\sum_{n=-\infty}^{\infty}(-1)^n\left\{1 + \cot h(\theta + 2\pi m)\frac{w}{L}\right\}\right.$$

$$\left. X\left\{\frac{\sin(\theta + 2\pi m)\frac{\ell}{2L}}{(\theta + 2\pi m)\frac{\ell}{2L}}\right\}\quad\left\{\frac{\sin(\theta + 2\pi m)\frac{L-\ell}{2L}}{(\theta + 2\pi m)\frac{L-\ell}{2L}}\right\}\right. \qquad \text{(III-14)}$$

If the ground plane is withdrawn $w \to \infty$ and we have

$$Y(\theta) = \sqrt{\frac{\epsilon}{\mu}}\left[\frac{4d}{\ell}\sin^2\frac{\theta}{2} + 4\frac{L-\ell}{L}\sin\frac{\theta}{2}\,S(\alpha)\right]$$

where $\alpha = \frac{\ell}{L}$ and

$$S(\alpha) = \sum_{n=-\alpha}^{\alpha}(-1)^n\left[\frac{\sin(\theta + 2\pi m)\frac{\ell}{2L}}{(\theta + 2\pi m)\frac{\ell}{2L}}\right]\left[\frac{\sin(\theta + 2\pi m)\frac{L-\ell}{2L}}{(\theta + 2\pi m)\frac{L-\ell}{2L}}\right]$$

which are equations (35) and (36). The opposite sense of circular polarization of the magnetic field above and below the plane of the fingers can be seen from equations (III-8, 9) and (III-11, 12).